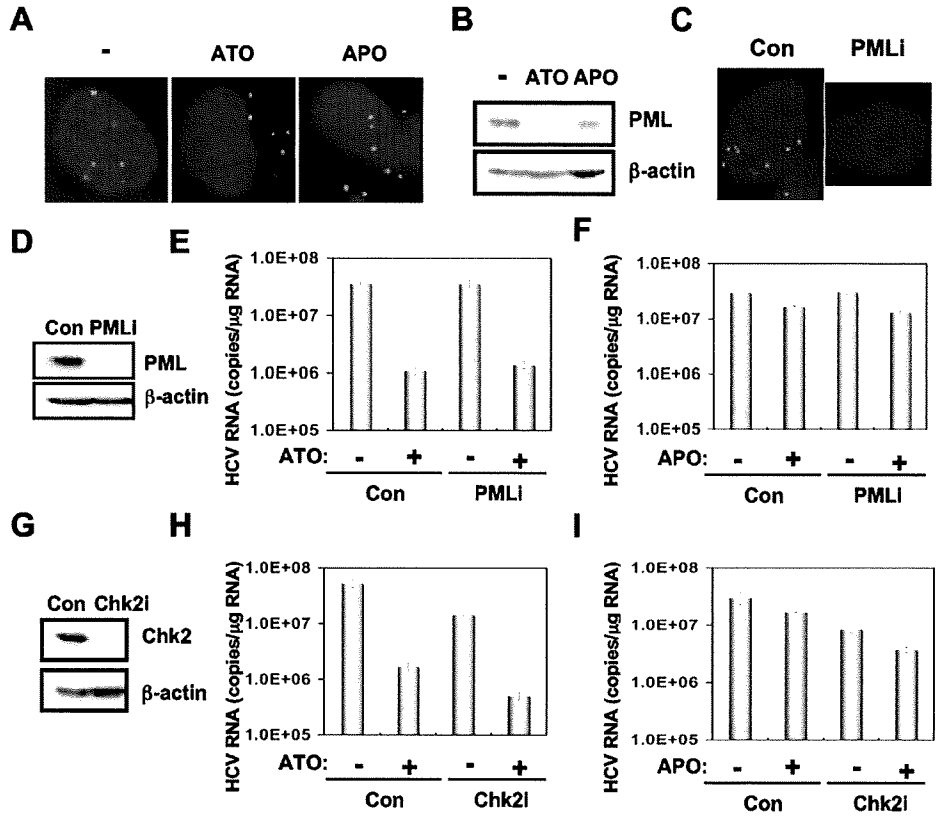

FIG. 4. PML and Chk2 are not required for the anti-HCV activity of ATO. (A) Subcellular localization of PML in O cells at 72 h after treatment with 10 μM NaOH (−), 1 μM ATO, or 1 μM APO. PML was detected by indirect immunofluorescence analysis with anti-PML antibody (PM001). DAPI staining of the nuclear DNA is also shown. (B) Induction of PML degradation by ATO but not by APO. The results of Western blot analysis of cellular lysates of O cells at 72 h after treatment with 10 μM NaOH (−), 1 μM ATO, or 1 μM APO with anti-PML (A301-168A-1) or anti-β-actin antibody are shown. (C) Stable knockdown of PML by shRNA-producing lentiviral vector in O cells. PML was detected by indirect immunofluorescence analysis with anti-PML antibody (PM001) in O cells expressing shRNA targeted to PML (PMLi) as well as in O cells transduced with a control lentiviral vector (Con). (D) Western blot analysis of cellular lysates with anti-PML (A301-168A-1) or anti-β-actin antibody in PML knockdown O cells (PMLi) as well as in control O cells (Con). (E and F) The level of genome-length HCV-O RNA was monitored by real-time LightCycler PCR in PML knockdown O cells (PMLi) as well as in control O cells (Con) after treatment with 10 μM NaOH (−), 1 μM ATO (+) (E), or 1 μM APO (+) (F) for 72 h. Results from three independent experiments conducted as described in the legend to Fig. 1A are shown. (G) Inhibition of Chk2 expression by shRNA-producing lentiviral vector. The results of Western blot analysis of cellular lysates with anti-Chk2 or anti-β-actin antibody in O cells expressing shRNA targeted to Chk2 (Chk2i) as well as in O cells transduced with a control lentiviral vector (Con) are shown. (H and I) The level of genome-length HCV-O RNA was monitored by real-time LightCycler PCR in Chk2 knockdown O cells (Chk2i) as well as in control O cells (Con) after treatment with 10 μM NaOH (−), 1 μM ATO (+) (H), or 1 μM APO (+) (I) for 72 h. Results from three independent experiments conducted as described in the legend to Fig. 1A are shown.

either 100 μM vitamin C or 10 mM NAC alone for 24 h or 72 h, the HCV replication was slightly enhanced (Fig. 6A and B), indicating that the antioxidant can activate HCV replication. Although the anti-HCV activity in the OR6 cells treated with 1 μM ATO and in combination with 100 μM vitamin C for 24 h was weakly reduced, 10 mM NAC completely and partially eliminated the anti-HCV activity of ATO after 24 h (Fig. 6A) and 72 h (Fig. 6B) of treatment, respectively, suggesting that oxidative stress and the glutathione redox system are associated with the anti-HCV activity of ATO. In contrast, the iNOS inhibitor 1400W did not suppress the HCV RNA replication or eliminate the anti-HCV activity of ATO, suggesting that NO is not involved in the anti-HCV activity of ATO (Fig. 6C). To further examine the involvement of oxidative stress in the anti-HCV activity of ATO, we examined ROS production in ATO-treated cells using two oxidative-sensitive fluorescent probes, DHE for detection of intracellular O_2^- and DCF for detection of intracellular H_2O_2. We found that 1 μM ATO could generate a significant level of intracellular O_2^- but not intracellular H_2O_2, while 2 μM BSO, an inhibitor of glutathione synthesis (14, 20, 33), could induce both O_2^- and H_2O_2 (Fig. 6D to H). Importantly, NAC diminished the ATO-dependent O_2^- induction (Fig. 6F). Since glutathione is a major antioxidant in cells and can clear away superoxide anion free radical, we also analyzed the changes of the intracellular glutathione level in ATO-treated O cells using CMF fluorescence, which can react with glutathione. As a result, we observed significant glutathione depletion in the cells treated with at least 1 μM ATO (Fig. 6I). To further confirm the involvement of glutathione in the anti-HCV activity of ATO, we examined the effect of cotreatment with ATO and BSO. When the OR6 cells were treated with 1 μM BSO alone, the HCV replication

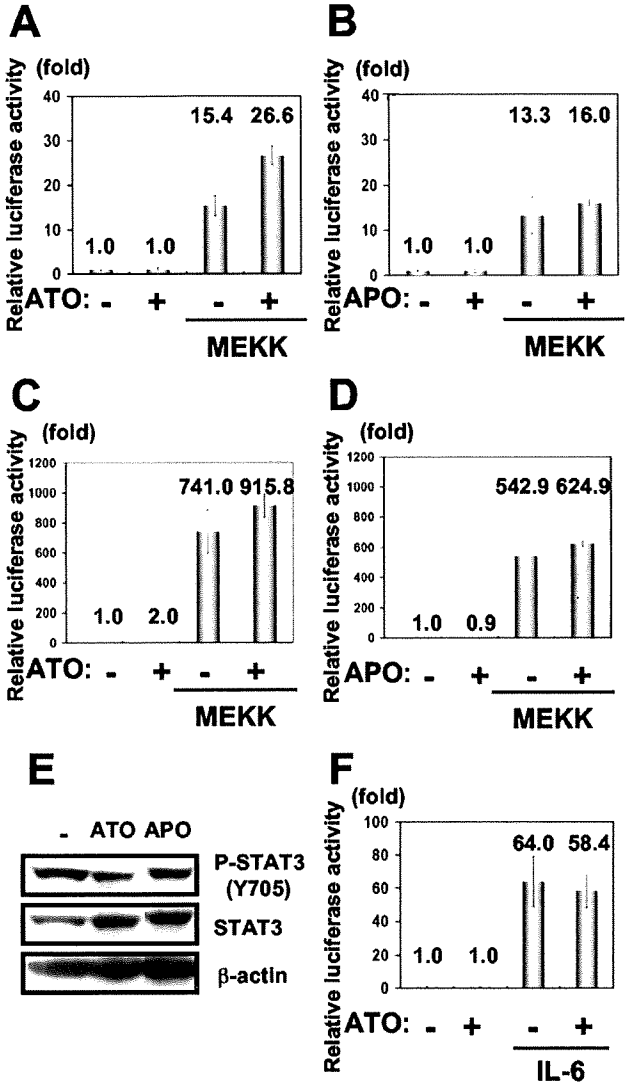

FIG. 5. Effect of ATO on the stress-signaling pathways. (A and B) Effect of ATO or APO on the NF-κB signaling pathway. O cells were transfected with 100 ng of reporter plasmid, pNF-κB-Luc, and/or 100 ng of pFC-MEKK (Stratagene, La Jolla, CA). Cells were treated with either 1 μM ATO (A) or 1 μM APO (B), and an FL assay was performed 24 h later. The results shown are means from three independent experiments. The relative FL activity is shown. (C and D) Effect of ATO or APO on the AP-1 signaling pathway. O cells were transfected with 100 ng of pAP-1-Luc and/or 100 ng of pFC-MEKK (Stratagene). Cells were treated with either 1 μM ATO (C) or 1 μM APO (D), and an FL assay was performed 24 h later as described for panels A and B. (E) Effect of ATO on the phosphorylation level of STAT3 at tyrosine 705. The results of Western blot analysis of cellular lysates with anti-phospho-STAT3 (Tyr705), anti-STAT3, or anti-β-actin antibody in O cells treated with either 1 μM ATO or 1 μM APO for 24 h are shown. (F) Effect of ATO on the STAT3 signaling pathway. O cells were transfected with 100 ng of STAT3 reporter APRE-Luc (41) (STAT3-Luc, a generous gift from T. Hirano, Osaka University, Japan). Cells were treated with 1 μM ATO for 19 h and then stimulated with 100 ng/ml of interleukin-6 for 5 h, and an FL assay was performed as described for panels A and B.

level was suppressed by about 30% compared with that of the control cells, and this occurred without cell toxicity (data not shown). However, consistent with previous reports in which ATO-induced apoptosis was enhanced by BSO (14, 20, 33), most of the cells died, possibly through apoptosis, when the OR6 cells were cotreated with 1 μM ATO and 1 μM BSO for 72 h (data not shown), suggesting that ATO and BSO synergistically generate ROS and deplete glutathione, resulting in induction of oxidative damage. Taken together, these results suggest that ATO may inhibit the HCV RNA replication by modulating the glutathione redox system and oxidative stress.

DISCUSSION

ATO has been reported to affect multiple biological functions, such as PML-NB formation, apoptosis, differentiation, stress response, and viral infection (38). Indeed, ATO has been shown to increase retroviral infectivity, including infectivity of HIV-1, HIV-2, feline immunodeficiency virus, simian immunodeficiency virus from rhesus macaques, and murine leukemia virus, although the mechanisms responsible for these changes are not well understood (5, 6, 32, 44, 47, 50, 57). PML, which is involved in host antiviral defenses, is required for the formation of the PML-NB, which is often disrupted or sequestered in the cytoplasm by infection with DNA or RNA viruses (17). The fact that ATO promotes the degradation of PML and alters the morphology or distribution of PML-NBs suggests that ATO enhances HIV-1 infection by antagonizing an antiviral activity associated with PML. In fact, HIV-1 infection has been reported to alter PML localization (57), although others have failed to confirm this finding (5). Furthermore, Berthoux et al. demonstrated that ATO stimulated retroviral reverse transcription (5). Moreover, ATO has been shown to have an inhibitory effect on host restriction factors, such as TRIM5α, Ref1, and Lv1, in a cell type-dependent manner (5, 6, 32, 44, 47, 50). In contrast, we have demonstrated that ATO strongly inhibited genome-length HCV RNA replication without cell toxicity (Fig. 1A and 2A). In addition, we observed the cytoplasmic translocation of PML in the HCV RNA-replicating O cells after the treatment with ATO (Fig. 4A). However, PML was dispensable for the anti-HCV activity of ATO as well as HCV RNA replication (Fig. 4E). In this regard, it is worth noting the recent report by Herzer et al. that the HCV core protein interacts with PML isoform IV and abrogates the PML function (22). Thus, PML may be involved in the HCV life cycle. In any case, the sensitivity to ATO and the cellular target of ATO seem to be different between HCV and HIV-1.

HCV infection has been shown to cause a state of chronic oxidative stress like that seen in chronic hepatitis C, which may contribute to fibrosis and carcinogenesis in the liver (16, 18, 40). In particular, HCV replication has been associated with the endoplasmic reticulum (ER), where HCV causes ER stress. Indeed, HCV NS5A and core, the ER-associated proteins, have been reported to trigger ER stress (4, 55). Therefore, HCV infection causes production of ROS and lowering of mitochondrial transmembrane potential through calcium signaling (4, 36). Among the HCV proteins, core, E1, NS3, and NS5A have been shown to be potent ROS inducers, and these HCV proteins also alter intracellular calcium levels and induce oxidative stress, thereby inducing DNA damage, and constitu-

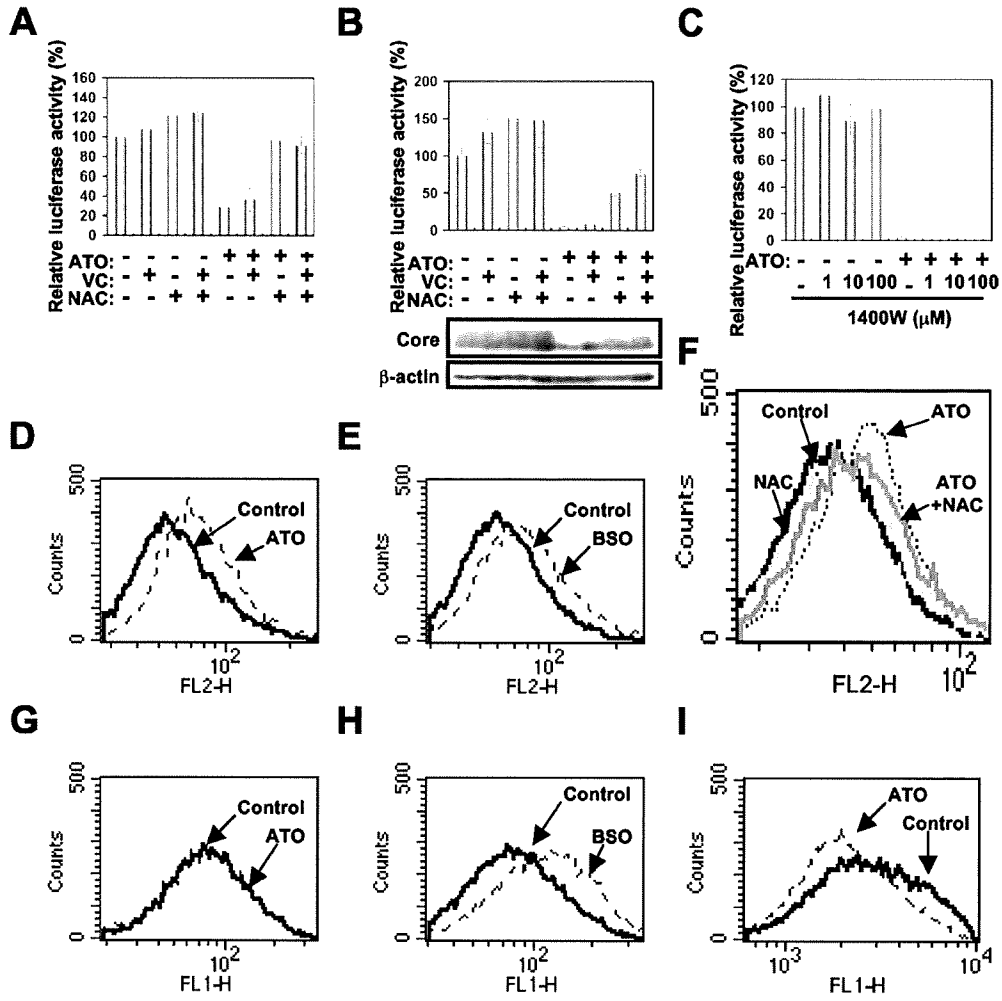

FIG. 6. The anti-HCV activity of ATO is associated with the glutathione redox system and oxidative stress. (A and B) The anti-HCV activity of ATO is eliminated by treatment with the antioxidant NAC. OR6 cells were treated with 1 μM ATO alone and in combination with 100 μM vitamin C (VC), with or without 10 mM NAC, for 24 h (A) or 72 h (B). The replication level of HCV RNA was monitored by the RL assay. The relative RL activity is shown. The results shown are means from three independent experiments; error bars indicate standard deviations. The results of Western blot analysis of cellular lysates with anti-HCV core or anti-β-actin antibody in OR6 cells at 72 h after the treatment with 1 μM ATO alone and in combination with 100 μM VC, with or without 10 mM NAC, are also shown. (C) Effect of combination treatment with ATO and the iNOS inhibitor 1400W on HCV RNA replication. OR6 cells were treated with 1 μM ATO alone and in combination with 1400W at the indicated concentrations for 72 h. The replication level of HCV RNA was monitored by the RL assay as described for panels A and B. (D and E) Effect of ATO on production of a ROS, O_2^-, in O cells. O cells were treated with 1 μM ATO (D) or 2 μM BSO (E) for 24 h. The intracellular O_2^- level was measured by flow cytometry using DHE as described in Materials and Methods. (F) Inhibition of ATO-dependent O_2^- induction by NAC. O cells were treated with either 1 μM ATO or 10 mM NAC alone and in combination with 10 mM NAC for 24 h. (G and H) Effect of ATO on production of a ROS, H_2O_2, in O cells. O cells were treated with 1 μM ATO (G) or 2 μM BSO (H) for 24 h. The intracellular H_2O_2 level was measured by flow cytometry using DCF as described in Materials and Methods. (I) Effect of ATO on the intracellular glutathione level in O cells. O cells were treated with 1 μM ATO for 72 h. The intracellular glutathione level was measured by flow cytometry using CellTracker Green CMFDA as described in Materials and Methods.

tively activate STAT3 and NF-κB, which are associated with HCV pathogenesis (19, 34, 36, 43, 49, 59, 60, 67). In fact, oxidative stress has been shown to trigger STAT3 tyrosine phosphorylation and nuclear translocation, which correlate with the activation of STAT3, leading to its DNA-binding activity (9). In contrast, ATO inhibited the STAT3 tyrosine phosphorylation through direct interaction with JAK kinase, thereby suppressing the transcriptional activity of STAT3 (12, 62). Importantly, STAT3 activation has been reported to be associated with HCV RNA replication (59, 69). The STAT3 Tyr705 dominant negative mutant has been shown to inhibit HCV RNA replication, suggesting that STAT3 positively regulates HCV replication (59). In contrast, others have reported that STAT3 induces anti-HCV activity (69). In this study, we analyzed the potential effect of ATO treatment on a set of stress-signaling events, including the NF-κB, AP-1, and STAT3 pathways, since ATO is known to modulate various signaling pathways. However, at 1 μM, which exerted an anti-HCV activity, the respective signaling pathways were not affected, arguing that the anti-HCV activity is independent of these

pathways (Fig. 5). In this regard, these stress-signaling pathways have been reported to be constitutively activated in HCV core- or NS5A-expressing cells (19, 36, 49, 59, 60, 67). In addition, previous studies demonstrated that ATO modulates the NF-κB, AP-1, and STAT3 pathways at higher concentrations (NF-κB, >10 μM; AP-1, >30 μM; STAT3, >4 μM). Therefore, we may have only observed the marginal effect of ATO in this study (Fig. 5). On the other hand, the HCV core or NS3 protein as well as HCV infection induces NO, leading to induction of double-stranded DNA breaks and accumulation of mutations of cellular genes (35). However, the iNOS inhibitor 1400W could not suppress HCV RNA replication and the anti-HCV activity of ATO, indicating that NO is not associated with the anti-HCV activity or with HCV replication (Fig. 6C).

It has been indicated that oxidative damage plays an important role in the effect of ATO (38). ROS generated in response to ATO exposure lead to accumulation of intracellular H_2O_2. Glutathione peroxidase and catalase are key enzymes regulating the levels of ROS and protecting cells from ATO-induced damage (26). However, the gastrointestinal glutathione peroxidase was drastically downregulated in cells harboring HCV replicons, which are rendered more susceptible to oxidative stress (39). The glutathione redox system has been implicated in the cellular defense system (14, 20). Glutathione, a major antioxidant in cells, is a tripeptide synthesized from cysteine, glutamic acid, and glycine, and it can scavenge superoxide anion free radicals. ATO has been shown to bind to the sulfhydryl group of glutathione and deplete the intracellular glutathione, resulting in enhancement of the sensitivity to oxidative damage (20, 33). Conversely, the antioxidant NAC is readily taken up by cells and serves as a precursor to elevate intracellular glutathione (53). In fact, ATO-induced apoptosis has been shown to be inhibited by NAC (11, 14, 21, 28). In this study, we have demonstrated that the anti-HCV activity of ATO was completely eliminated by treatment with NAC for 24 h (Fig. 6A). In addition, we found that ATO increased intracellular O_2^- but not H_2O_2 and depleted the intracellular glutathione in HCV RNA-replicating cells (Fig. 6D to I). Importantly, NAC diminished the ATO-dependent O_2^- induction (Fig. 6F). This finding could strengthen the link between ATO-dependent oxidative stress and anti-HCV activity. Similarly, Wen et al. reported an increase in ROS and enhanced susceptibility to glutathione depletion in the HCV core-expressing HepG2 cells (61). Accordingly, ROS have been shown to significantly suppress RNA replication in HCV replicon-harboring cells treated with H_2O_2 (13). In addition, HCV replication has been shown to be inhibited by lipid peroxidation of arachidonate, and this peroxidation could be blocked by lipid-soluble antioxidants such as vitamin E (23). Conversely, several antioxidants, such as vitamin C, vitamin E, and NAC, enhanced HCV replication in the present study (Fig. 6A and B) (65). Thus, we suggest that ATO inhibited HCV RNA replication by modulating the glutathione redox system and oxidative stress. In contrast to the above findings with HCV, NAC has been shown to suppress HIV-1 replication by preventing the activation of HIV-1 long terminal repeat transcription by NF-κB, suggesting a correlation between a decrease in glutathione levels and activation of HIV-1 replication (46, 53, 54). In this context, ATO has shown opposite effects on HIV-1 and HCV replication, stimulating the former and inhibiting the latter. Considering all of these results together, ATO can be regarded as a useful, novel anti-HCV reagent. In addition, the host redox system may be critical for HCV replication and may represent a pivotal target for the clinical treatment of patients with chronic hepatitis C.

ACKNOWLEDGMENTS

We thank D. Trono, R. Agami, R. Iggo, A. Takamizawa, T. Hirano, A. Yoshimura, and M. Hijikata for the VSV G-pseudotyped HIV-1-based vector system pCMVΔR8.91, pMDG2, pSUPER, pRDI292, anti-NS5A antibody, APRE-Luc, and 293FT cells. We also thank T. Stamminger, M. Yano, and T. Nakamura for their helpful suggestions and technical assistance.

This work was supported by a Grant-in-Aid for Scientific Research (C) from the Japan Society for the Promotion of Science (JSPS); by a Grant-in-Aid for Research on Hepatitis from the Ministry of Health, Labor, and Welfare of Japan; by the Kawasaki Foundation for Medical Science and Medical Welfare; by the Okayama Medical Foundation; and by the Ryobi Teien Memorial Foundation.

REFERENCES

1. **Ariumi, Y., T. Priscilla, M. Masutani, and D. Trono.** 2005. DNA damage sensors ATM, ATR, DNA-PKcs, and PARP-1 are dispensable for human immunodeficiency virus type 1 integration. J. Virol. **79**:2973–2978.
2. **Ariumi, Y., M. Kuroki, K. Abe, H. Dansako, M. Ikeda, T. Wakita, and N. Kato.** 2007. DDX3 DEAD-box RNA helicase is required for hepatitis C virus RNA replication. J. Virol. **81**:13922–13926.
3. **Ariumi, Y., M. Kuroki, H. Dansako, K. Abe, M. Ikeda, T. Wakita, and N. Kato.** 2008. The DNA damage sensors, ataxia-telangiectasia mutated kinase and checkpoint kinase 2 are required for hepatitis C virus RNA replication. J. Virol. **82**:9639–9646.
4. **Benali-Furet, N. L., M. Chami, L. Houel, F. De Giorgi, F. Vernejoul, D. Lagorce, L. Buscail, R. Bartenschlager, F. Ichas, R. Rizzuto, and P. Paterlini-Bréchot.** 2005. Hepatitis C virus core triggers apoptosis in liver cells by inducing ER stress and ER calcium depletion. Oncogene **24**:4921–4933.
5. **Berthoux, L., G. J. Towers, C. Gurer, P. Salomoni, P. P. Pandolfi, and J. Luban.** 2003. As2O3 enhances retroviral reverse transcription and counteracts Ref1 antiviral activity. J. Virol. **77**:3167–3180.
6. **Berthoux, L., S. Sebastian, E. Sokolskaja, and J. Luban.** 2004. Lv1 inhibition of human immunodeficiency virus type 1 is counteracted by factors that stimulate synthesis or nuclear translocation of viral cDNA. J. Virol. **78**: 11739–11750.
7. **Bridge, A. J., S. Pebernard, A. Ducraux, A. L. Nicoulaz, and R. Iggo.** 2003. Induction of an interferon response by RNAi vectors in mammalian cells. Nat. Genet. **34**:263–264.
8. **Brummelkamp, T. R., R. Bernard, and R. Agami.** 2002. A system for stable expression of short interfering RNAs in mammalian cells. Science **296**:550–553.
9. **Carballo, M., M. Conde, R. E. Bekay, J. Martín-Nieto, M. J. Camacho, J. Monteseirín, J. Conde, F. J. Bedoya, and F. Sobrino.** 1999. Oxidative stress triggers STAT3 tyrosine phosphorylation and nuclear translocation in human lymphocytes. J. Biol. Chem. **274**:17580–17586.
10. **Cavigelli, M., W. W. Li, A. Lin, B. Su, K. Yoshioka, and M. Karin.** 1996. The tumor promoter arsenite stimulates AP-1 activity by inhibiting a JNK phosphatase. EMBO J. **15**:6269–6279.
11. **Chen, Y. C., S. Y. Lin-Shiau, and J. K. Lin.** 1998. Involvement of reactive oxygen species and caspase 3 activation in arsenite-induced apoptosis. J. Cell Physiol. **177**:324–333.
12. **Cheng, H. Y., P. Li, M. David, T. E. Smithgall, L. Feng, and M. W. Lieberman.** 2004. Arsenic inhibition of the JAK-STAT pathway. Oncogene **23**: 3603–3612.
13. **Choi, J., K. J. Lee, Y. Zheng, A. K. Yamaga, M. M. C. Lai, and J. H. Ou.** 2004. Reactive oxygen species suppress hepatitis C virus RNA replication in human hepatoma cells. Hepatology **39**:81–89.
14. **Dai, J., R. S. Weinberg, S. Waxman, and Y. Jing.** 1999. Malignant cells can be sensitized to undergo growth inhibition and apoptosis by arsenic trioxide through modulation of the glutathione redox system. Blood **93**:268–277.
15. **Davis, G. L.** 2006. Tailoring antiviral therapy in hepatitis C. Hepatology **43**:909–911.
16. **De Maria, N., A. Colantoni, S. Fagiuoli, G. J. Liu, B. K. Rogers, F. Farinati, D. H. Van Thiel, and R. A. Floyd.** 1996. Association between reactive oxygen species and disease activity in chronic hepatitis C. Free Radic. Biol. Med. **21**:291–295.
17. **Everett, R. D., and M. K. Chelbi-Alix.** 2007. PML and PML nuclear bodies: implications in antiviral defence. Biochemie **89**:819–830.
18. **Farinati, F., R. Cardin, N. De Maria, G. D. Libera, C. Marafin, E. Lecis, P.**

Burra, A. Floreani, A. Cecchetto, and R. Naccarato. 1995. Iron storage, lipid peroxidation and glutathione turnover in chronic anti-HCV positive hepatitis. J. Hepatol. **22**:449–456.
19. **Gong, G., G. Waris, R. Tanveer, and A. Siddiqui.** 2001. Human hepatitis C virus NS5A protein alters intracellular calcium levels, induces oxidative stress, and activates STAT-3 and NF-κB. Proc. Natl. Acad. Sci. USA **98**: 9599–9604.
20. **Han, Y. H., S. H. Kim, S. Z. Kim, and W. H. Park.** 2008. Apoptosis in arsenic trioxide-treated Calu-6 lung cells is correlated with the depletion of GSH levels rather than the change of ROS levels. J. Cell. Biochem. **104**:862–878.
21. **Han, Y. H., S. Z. Kim, S. H. Kim, and W. H. Park.** 2008. Suppression of arsenic trioxide-induced apoptosis in HeLa cells by N-acetylcysteine. Molecules Cells **26**:18–25.
22. **Herzer, K., S. Weyer, P. H. Krammer, P. R. Galle, and T. G. Hofmann.** 2005. Hepatitis C virus core protein inhibits tumor suppressor protein promyelocytic leukemia function in human hepatoma cells. Cancer Res. **65**:10830–10837.
23. **Huang, H., Y. Chen, and J. Ye.** 2007. Inhibition of hepatitis C virus replication by peroxidation of arachidonate and restoration by vitamin E. Proc. Natl. Acad. Sci. USA **104**:18666–18670.
24. **Hwang, D. R., Y. C. Tsai, J. C. Lee, K. K. Huang, R. K. Lin, C. H. Ho, J. M. Chiou, Y. T. Lin, J. T. A. Hsu, and C. T. Yeh.** 2004. Inhibition of hepatitis C virus replication by arsenic trioxide. Antimicrob. Agents Chemother. **48**: 2876–2882.
25. **Ikeda, M., K. Abe, H. Dansako, T. Nakamura, K. Naka, and N. Kato.** 2005. Efficient replication of a full-length hepatitis C virus genome, strain O, in cell culture, and development of a luciferase reporter system. Biochem. Biophys. Res. Commun. **329**:1350–1359.
26. **Jing, Y., J. Dai, R. M. E. Chalmers-Redman, W. G. Tatton, and S. Waxman.** 1999. Arsenic trioxide selectively induces acute promyelocytic leukemia cell apoptosis via a hydrogen peroxide-depndent pathway. Blood **94**:2102–2111.
27. **Joe, Y., J. H. Jeong, S. Yang, H. Kang, N. Motoyama, P. P. Pandolfi, J. H. Chung, and M. K. Kim.** 2006. ATR, PML, and Chk2 play a role in arsenic trioxide-induced apoptosis. J. Biol. Chem. **281**:28764–28771.
28. **Kang, Y. H., M. J. Yi, M. J. Kim, M. T. Park, S. Bae, C. M. Kang, C. K. Cho, I. C. Park, M. J. Park, C. H. Rhee, S. I. Hong, H. Y. Chung, Y. S. Lee, and S. J. Lee.** 2004. Caspase-independent cell death by arsenic trioxide in human cervical cancer cells: reactive oxygen species-mediated poly(ADP-ribose) polymerase-1 activation signals apoptosis-inducing factor release from mitochondria. Cancer Res. **64**:8960–8967.
29. **Kapahi, P., T. Takahashi, G. Natoli, S. R. Adams, Y. Chen, R. Y. Tsien, and M. Karin.** 2000. Inhibition of NF-κB activation by arsenite through reaction with a critical cysteine in the activation loop of IκB kinase. J. Biol. Chem. **275**:36062–36066.
30. **Kato, N.** 2001. Molecular virology of hepatitis C virus. Acta Med. Okayama **55**:133–159.
31. **Kato, N., K. Sugiyama, K. Namba, H. Dansako, T. Nakamura, M. Takami, K. Naka, A. Nozaki, and K. Shimotohno.** 2003. Establishment of a hepatitis C virus subgenomic replicon derived from human hepatocytes infected in vitro. Biochem. Biophys. Res. Commun. **306**:756–766.
32. **Keckesova, Z., L. M. J. Ylinen, and G. J. Towers.** 2004. The human and African green monkey TRIM5α genes encode Ref1 and Lv1 retroviral restriction factor activities. Proc. Natl. Acad. Sci. USA **101**:10780–10785.
33. **Kito, M., Y. Akao, N. Ohishi, K. Yagi, and Y. Nozawa.** 2002. Arsenic trioxide-induced apoptosis and its enhancement by buthionine sulfoximine in hepatocellular carcinoma cell lines. Biochem. Biophys. Res. Commun. **291**:861–867.
34. **Korenaga, M., T. Wang, Y. Li, L. A. Showalter, T. Chan, J. Sun, and S. A. Weinman.** 2005. Hepatitis C virus core protein inhibits mitochondrial electron transport and increases reactive oxygen species (ROS) production. J. Biol. Chem. **280**:37481–37488.
35. **Machida, K., K. T. Cheng, V. M. Sung, K. J. Lee, A. M. Levine, and M. M. C. Lai.** 2004. Hepatitis C virus infection activates the immunologic (type II) isoform of nitric oxide synthase and thereby enhances DNA damage and mutations of cellular genes. J. Virol. **78**:8835–8843.
36. **Machida, K., K. T. H. Cheng, C. K. Lai, K. S. Jeng, V. M. H. Sung, and M. M. C. Lai.** 2006. Hepatitis C virus triggers mitochondrial permeability transition with production of ractive oxygen species, leading to DNA damage and STAT3 activation. J. Virol. **80**:7199–7207.
37. **Meyer, M., R. Schreck, and P. A. Baeuerle.** 1993. H_2O_2 and antioxidants have opposite effects on activation of NF-κB and AP-1 in intact cells: AP-1 as secondary antioxidant-responsive factor. EMBO J. **12**:2005–2015.
38. **Miller, W. H., Jr., H. M. Schipper, J. S. Lee, J. Singer, and S. Waxman.** 2002. Mechanisms of action of arsenic trioxide. Cancer Res. **62**:3893–3903.
39. **Morbitzer, M., and T. Herget.** 2005. Expression of gastrointestinal glutathione peroxidase is inversely correlated to the presence of hepatitis C virus subgenomic RNA in human liver cells. J. Biol. Chem. **280**:8831–8841.
40. **Moriya, K., K. Nakagawa, T. Santa, Y. Shintani, H. Fujie, H. Miyoshi, T. Tsutsumi, T. Miyazawa, K. Ishibashi, T. Horie, K. Imai, T. Todoroki, S. Kimura, and K. Koike.** 2001. Oxidative stress in the absence of inflammation in a mouse model for hepatitis C virus-associated hepatocarcinogenesis. Cancer Res. **61**:4365–4370.
41. **Nakajima, K., Y. Yamanaka, K. Nakae, H. Kojima, M. Ichiba, N. Kiuchi, T. Kitaoka, T. Fukada, M. Hibi, and T. Hirano.** 1996. A central role for STAT3 in IL-6-induced regulation of growth and differentiation in M1 leukemia cells. EMBO J. **15**:3651–3658.
42. **Naldini, L., U. Blömer, P. Gallay, D. Ory, R. Mulligan, F. H. Gage, I. M. Verma, and D. Trono.** 1996. In vivo gene delivery and stable transduction of nondividing cells by a lentiviral vector. Science **272**:263–267.
43. **Okuda, M., K. Li, M. R. Beard, L. A. Showalter, F. Scholle, S. M. Lemon, and S. A. Weinman.** 2002. Mitochondrial injury, oxidative stress, and antioxidant gene expression are induced by hepatitis C virus core protein. Gastroenterology **122**:366–375.
44. **Pion, M., R. Stalder, R. Correa, B. Mangeat, G. J. Towers, and V. Piguet.** 2007. Identification of an arsenic-sensitive block to primate lentiviral infection of human dendritic cells. J. Virol. **81**:12086–12090.
45. **Porter, A. C., G. R. Fanger, and R. R. Vaillancourt.** 1999. Signal transduction pathways regulated by arsenate and arsenite. Oncogene **18**:7794–7802.
46. **Roederer, M., F. J. T. Staal, P. A. Raju, S. W. Ela, L. A. Herzenberg, and L. A. Herzenberg.** 1990. Cytokine-stimulated human immunodeficiency virus replication is inhibited by *N*-acetyl-L-cysteine. Proc. Natl. Acad. Sci. USA **87**:4884–4888.
47. **Saenz, D. T., W. Teo, J. C. Olsen, and E. M. Poeschla.** 2005. Restriction of feline immunodeficiency virus by Ref1, Lv1, and primate TRIM5α proteins. J. Virol. **79**:15175–15188.
48. **Sakurai, T., T. Kaise, and C. Matsubara.** 1998. Inorganic and methylated arsenic compounds induce cell death in murine macrophages via different mechanisms. Chem. Res. Toxicol. **11**:273–283.
49. **Sarcar, B., A. K. Ghosh, R. Steele, R. Ray, and R. B. Ray.** 2004. Hepatitis C virus NS5A mediated STAT3 activation requires co-operation of Jak1 kinase. Virology **322**:51–60.
50. **Sayah, D. M., and J. Luban.** 2004. Selection for loss of Ref1 activity in human cells releases human immunodeficiency virus type 1 from cyclophilin A dependence during infection. J. Virol. **78**:12066–12070.
51. **Shen, Z. X., G. Q. Chen, J. H. Ni, X. S. Li, S. M. Xiong, Q. Y. Qiu, J. Zhu, W. Tang, G. L. Sun, K. Q. Yang, Y. Chen, L. Zhou, Z. W. Fang, Y. T. Wang, J. Ma, P. Zhang, T. D. Zhang, S. J. Chen, Z. Chen, and Z. Y. Wang.** 1997. Use of arsenic trioxide (As_2O_3) in the treatment of acute promyelocytic leukemia (APL). II. Clinical efficacy and pharmacokinetics in relapsed patients. Blood **89**:3354–3360.
52. **Soignet, S. L., P. Maslak, Z. G. Wang, S. Jhanwar, E. Calleja, L. J. Dardashti, D. Corso, A. DeBlasio, J. Gabrilove, D. A. Scheinberg, P. P. Pandolfi, and R. P. Warrell, Jr.** 1998. Complete remission after treatment of acute promyelocytic leukemia with arsenic trioxide. N. Engl. J. Med. **339**:1341–1348.
53. **Staal, F. J. T., M. Roederer, L. A. Herzenberg, and L. A. Herzenberg.** 1990. Intracellular thiols regulate activation of nuclear factor κB and transcription of human immunodeficiency virus. Proc. Natl. Acad. Sci. USA **87**:9943–9947.
54. **Staal, F. J. T., S. W. Ela, M. Roederer, M. T. Anderson, L. A. Herzenberg, and L. A. Herzenberg.** 1992. Glutathione deficiency and human immunodeficiency virus infection. Lancet **339**:909–912.
55. **Tardif, K. D., K. Mori, and A. Siddiqui.** 2002. Hepatitis C virus subgenomic replicons induce endoplasmic reticulum stress activating an intracellular signaling pathway. J. Virol. **76**:7453–7459.
56. **Tavalai, N., P. Papior, S. Rechter, M. Leis, and T. Stamminger.** 2006. Evidence for a role of the cellular ND10 protein PML in mediating intrinsic immunity against human cytomegalovirus infections. J. Virol. **80**:8006–8018.
57. **Turelli, P., V. Doucas, E. Craig, B. Mangeat, N. Klages, R. Evans, G. Kalpana, and D. Trono.** 2001. Cytoplasmic recruitment of INI1 and PML on incoming HIV preintegration complexes: interference with early steps of viral replication. Mol. Cell **7**:1245–1254.
58. **Wakita, T., T. Pietschmann, T. Kato, T. Date, M. Miyamoto, Z. Zhao, K. Murthy, A. Habermann, H. G. Kräusslich, M. Mizokami, R. Bartenschlager, and T. J. Liang.** 2005. Production of infectious hepatitis C virus in tissue culture from a cloned viral genome. Nat. Med. **11**:791–796.
59. **Waris, G., J. Turson, T. Hassanein, and A. Siddiqui.** 2005. Hepatitis C virus (HCV) constitutively activates STAT-3 via oxidative stress: role of STAT3 in HCV replication. J. Virol. **79**:1569–1580.
60. **Waris, G., A. Livolsi, V. Imbert, J. F. Peyron, and A. Siddiqui.** 2003. Hepatitis C virus NS5A and subgenomic replicon activate NF-κB via tyrosine phosphorylation of IkBa and its degradation by calpain protease. J. Biol. Chem. **278**:40778–40787.
61. **Wen, F., M. Y. Abdalla, C. Aloman, J. Xiang, I. M. Ahmad, J. Walewski, M. L. McCormick, K. E. Brown, A. D. Branch, D. R. Spitz, B. E. Britigan, and W. N. Schmidt.** 2004. Increased prooxidant production and enhanced susceptibility to glutathione depletion in HepG2 cells co-expressing HCV core protein and CYP2E1. J. Med. Virol. **72**:230–240.
62. **Wetzler, M., M. T. Brady, E. Tracy, Z. R. Li, K. A. Donohue, K. L. O'Loughlin, Y. Cheng, A. Mortazavi, A. A. McDonald, P. Kunapuli, P. K. Wallace, M. R. Baer, J. K. Cowell, and H. Baumann.** 2006. Arsenic trioxide affects signal transducer and activator of transcription proteins through alteration of protein tyrosine kinase phosphorylation. Clin. Cancer Res. **12**: 6817–6825.

63. **Yang, S., C. Kuo, J. E. Bisi, and M. K. Kim.** 2002. PML-dependent apoptosis after DNA damage is regulated by the checkpoint kinase hCds1/Chk2. Nat. Cell Biol. **4**:865–870.
64. **Yang, S., J. H. Jeong, A. L. Brown, C. H. Lee, P. P. Pandolfi, J. H. Chung, and M. K. Kim.** 2006. Promyelocytic leukemia activates Chk2 by mediating Chk2 autophosphorylation. J. Biol. Chem. **281**:26645–26654.
65. **Yano, M., M. Ikeda, K. Abe, H. Dansako, S. Ohkoshi, Y. Aoyagi, and N. Kato.** 2007. Comprehensive analysis of the effects of ordinary nutrients on hepatitis C virus RNA replication in cell culture. Antimicrob. Agents Chemother. **51**:2016–2027.
66. **Yoda, A., K. Toyoshima, Y. Watanabe, N. Onishi, Y. Hazaka, Y. Tsukuda, J. Tsukada, T. Kondo, Y. Tanaka, and Y. Minami.** 2008. Arsenic trioxide augments Chk2/p53-mediated apoptosis by inhibiting oncogenic Wip1 phosphatase. J. Biol. Chem. **283**:18969–18979.
67. **Yoshida, T., T. Hanada, T. Tokuhisa, K. Kosai, M. Sata, M. Kohara, and A. Yoshimura.** 2002. Activation of STAT3 by the hepatitis C virus core protein leads to cellular transformation. J. Exp. Med. **196**:641–653.
68. **Zhang, P., S. Y. Wang, and X. H. Hu.** 1996. Arsenic trioxide treated 72 cases of acute promyelocytic leukemia. Chin. J. Hematol. **17**:58–62.
69. **Zhu, H., X. Shang, N. Terada, and C. Liu.** 2004. STAT3 induces anti-hepatitis C viral activity in liver cells. Biochem. Biophys. Res. Commun. **324**:518–528.
70. **Zhu, J., M. H. M. Koken, F. Quignon, M. K. Chelbi-Alix, L. Degos, Z. Y. Wang, Z. Chen, and H. de Thé.** 1997. Arsenic-induced PML targeting onto nuclear bodies: implications for the treatment of acute promyelocytic leukemia. Proc. Natl. Acad. Sci. USA **94**:3978–3983.
71. **Zufferey, R., D. Nagy, R. J. Mandel, L. Naldini, and D. Trono.** 1997. Multiply attenuated lentiviral vector achieves efficient gene delivery in vivo. Nat. Biotechnol. **15**:871–875.

The American Journal of Pathology, Vol 171, No 3, September 2007

DOI 10.2353/ajpath.2007.060972

Gastrointestinal, Hepatobiliary and Pancreatic Pathology

Oncostatin M Gene Therapy Attenuates Liver Damage Induced by Dimethylnitrosamine in Rats

Tetsuhiro Hamada,*† Ayuko Sato,* Tadamichi Hirano,† Takashi Yamamoto,‡ Gakuhei Son,† Masayuki Onodera,* Ikuko Torii,* Takashi Nishigami,* Minoru Tanaka,§ Atsushi Miyajima,§ Shuhei Nishiguchi,¶ Jiro Fujimoto,† and Tohru Tsujimura*

From the Departments of Pathology and Surgery† and Division of Hepatobiliary and Pancreatic Medicine, Department of Internal Medicine,¶ Hyogo College of Medicine, Hyogo; the Department of Clinical Laboratory, Osaka Medical Center for Cancer and Cardiovascular Diseases,‡ Osaka, and the Institute of Molecular and Cellular Biosciences,§ University of Tokyo, Tokyo, Japan*

To assess the usefulness of oncostatin M (*osm*) gene therapy in liver regeneration, we examined whether the introduction of OSM cDNA enhances the regeneration of livers damaged by dimethylnitrosamine (DMN) in rats. Repeated injection of OSM cDNA enclosed in hemagglutinating virus of Japan envelope into the spleen resulted in the exclusive expression of OSM protein in Kupffer cells of the liver, which was accompanied by increases in body weight, liver weight, and serum albumin levels and the reduction of serum liver injury parameters (bilirubin, aspartate aminotransferase, and alanine aminotransferase) and a serum fibrosis parameter (hyaluronic acid). Histological examination showed that *osm* gene therapy reduced centrilobular necrosis and inflammatory cell infiltration and augmented hepatocyte proliferation. The apoptosis of hepatocytes and fibrosis were suppressed by *osm* gene therapy. Time-course studies on *osm* gene therapy before or after DMN treatment showed that this therapy was effective not only in enhancing regeneration of hepatocytes damaged by DMN but in preventing hepatic cytotoxicity caused by subsequent treatment with DMN. These results indicate that OSM is a key mediator for proliferation and anti-apoptosis of hepatocytes and suggest that *osm* gene therapy is useful, as preventive and curative means, for the treatment of patients with liver damage. (*Am J Pathol* 2007, 171:872–881; DOI: 10.2353/ajpath.2007.060972)

The liver has a remarkable ability to respond to injuries inflicted by various causes, such as partial hepatectomy, toxic exposure, and virus infection.[1,2] Hepatocytes, which are liver parenchymal cells and normally in the quiescent G_0 phase, re-enter the cell cycle after injury to restore its mass, architecture, and function. In this process, a number of growth factors and cytokines have been reported to be involved.[3–9] For example, hepatocyte growth factor (HGF) functions as a potent mitogen for hepatocytes,[10] and the administration of HGF has been shown to ameliorate hepatic injury in animal models of fulminant hepatic failure.[11–13] It has also been shown that the introduction of *hgf* gene into rat cirrhotic livers using liposome with the hemagglutinating virus of Japan (HVJ) inhibits fibrogenesis and hepatocyte apoptosis, leading to the complete resolution of fibrosis and improvement of survival rate.[14]

Oncostatin M (OSM) is a member of the interleukin (IL)-6 cytokine family that includes IL-6, IL-11, leukemia inhibitory factor, ciliary neurotrophic factor, cardiotrophin-1, and novel neutrophin-1/B-cell-stimulating factor-3.[15–18] Mouse OSM receptor is composed of the gp130 subunit, common to all of the IL-6 family cytokines, and an OSM-specific subunit (hereafter called OSM-specific receptor; OSM-R).[19] Binding of OSM to its receptor complex activates Janus tyrosine kinases (Jak1, Jak2, and Tyk2), which in turn activates downstream signaling pathways, including SHP-2 tyrosine phosphatase and signal transducer and activator of transcription protein 3 (STAT3). Recently, OSM has been shown to induce maturation of mouse hepatocytes derived from embryonic day 14.5 liver.[20] In addition, Nakamura and colleagues[21] have shown that OSM-R knockout (OSM-$R^{-/-}$) mice exhibit

Supported in part by the Ministry of Education, Science, Sports, Culture, and Technology of Japan (grants-in-aid for scientific research and Hitec Research Center grant) and Hyogo College of Medicine (grants-in-aid for promotion of core research projects, graduate students, and researchers)

Accepted for publication June 5, 2007.

Supplemental material for this article can be found on *http://ajp.amjpathol.org*.

Address reprint requests to Tohru Tsujimura, M.D., Ph.D., Department of Pathology, Hyogo College of Medicine, 1, Mukogawa, Nishinomiya, Hyogo 663-8501, Japan. E-mail: tohru@hyo-med.ac.jp.

delayed hepatocyte proliferation, persistent liver necrosis, and increased tissue destruction after CCl_4 treatment. They have also shown that the administration of OSM reduces CCl_4-induced acute liver failure in wild-type mice.[21] These results suggest that OSM, like HGF, plays an important role in liver regeneration.

Recently, we have succeeded in isolating rat OSM cDNA.[22] In this study, we examined whether the introduction of this OSM cDNA enhances liver regeneration and suppresses fibrogenesis in rats administrated with dimethylnitrosamine (DMN). Repeated injection of HVJ envelope complex[23] with rat OSM cDNA (hereafter called HVJ-OSM) into the spleen reduced centrilobular necrosis and inflammatory cell infiltration, induced hepatocyte proliferation, and suppressed hepatocyte apoptosis. Serum liver injury parameters, such as bilirubin, aspartate aminotransferase (AST), and alanine aminotransferase (ALT), and a fibrosis parameter, hyaluronic acid, were improved. In addition, *osm* gene therapy was effective in both protection against hepatic cytotoxicity caused by subsequent treatment with DMN and enhancement of regeneration of hepatocytes damaged by DMN. These results support a crucial role of OSM in liver regeneration and suggest that *osm* gene therapy is useful, as preventive and curative means, for the treatment of patients with liver damage.

Materials and Methods

Rats and Treatments

Male Sprague-Dawley rats of 4 weeks of age were purchased from Japan SLC (Hamamatsu, Shizuoka, Japan). To examine the effect of OSM cDNA introduction on the physiological condition of rats, we injected HVJ-OSM, prepared from pEF-BOS with rat OSM cDNA[22] by HVJ Envelope Vector kit (GenomONE-Neo; Ishihara Industry Corp., Osaka, Japan) according to the manufacturer's protocol, or the HVJ envelope complex without rat OSM cDNA (hereafter called HVJ-Vector) into rats (n = 12) weekly for 3 weeks. On the next day of the last injection, rats were sacrificed, blood was taken from the right ventricle of hearts, and sera were prepared and stored at −80°C until analysis. Livers were promptly removed to determine the weight and examine histology. Albumin, total bilirubin (T-Bil), direct bilirubin (D-Bil), AST, ALT, and hyaluronic acid in the sera were measured by standard laboratory techniques. Other rats were then divided into two groups. One group (n = 6) received *osm* gene therapy that was performed as follows. DMN (Sigma-Aldrich Co., St. Louis, MO) was given intraperitoneally at 15 mg/kg body weight for 3 consecutive days per week for 3 weeks to induce liver damage and fibrosis. On day 4 of each week, HVJ-OSM was injected into the spleen. The other group (n = 6) that served as control was treated with DMN similarly for 3 consecutive days per week for 3 weeks, and on day 4 of each week, HVJ-Vector was injected into the spleen. On day 5 of the last week, rats were sacrificed. For time-course studies on *osm* gene therapy before DMN treatment, HVJ-OSM or HVJ-Vector was injected into the spleens of rats (n = 18), and 24 hours later, DMN was given intraperitoneally at 21 mg/kg body weight. For time-course studies on *osm* gene therapy after DMN treatment, DMN was given intraperitoneally at 21 mg/kg body weight, and HVJ-OSM or HVJ-Vector was injected into the spleen of rats (n = 18) 24 hours later. In both experiments, rats were sacrificed every day. All surgical procedures on rats were done under pentobarbital sodium anesthesia. All experimental procedures were approved by the Animal Care Committee of Hyogo College of Medicine and performed in accordance with the criteria outlined in the "Guide for the Care and Use of Laboratory Animals" prepared by the National Academy of Science.

Histological Examination

The removed liver was fixed with methacarn (methanol/chloroform/glacial acetic acid, 6:3:1) or 10% formalin neutral buffer solution, embedded in paraffin, and cut into 5-μm-thick sections. For OSM immunostaining, sections were incubated with goat anti-mouse OSM antibody (R&D Systems, Minneapolis, MN) and then sequentially with horseradish peroxidase-conjugated donkey anti-goat IgG antibody (Santa Cruz Biotechnology, Santa Cruz, CA), biotinyl tyramine (DAKO, Glostrup, Denmark), and horseradish peroxidase-conjugated streptavidin (DAKO). For Ki-67 immunostaining, sections were heated in 10 mmol/L sodium citrate buffer (pH 6.0) at 95°C for 40 minutes to facilitate antigen retrieval. The sections were incubated with rabbit polyclonal antibody against human Ki-67 nuclear antigen (Novocastra Laboratories Ltd., Benton Lane, UK) and then with Histofine Simple Stain MAX-PO(R) (Nichirei Corporation, Tokyo, Japan). Immunoreacted cells for OSM and Ki-67 were visualized with Simple Stain DAB solution (Nichirei). The sections were lightly counterstained with hematoxylin. Total and Ki-67-positive hepatocytes were counted in 10 portal fields selected randomly in each specimen. Apoptotic hepatocytes were visualized by terminal dUTP nick-end labeling (TUNEL) staining using an apoptosis *in situ* detection kit (Wako Pure Chemical Industries, Ltd., Osaka, Japan). Apoptotic hepatocytes were counted in 10 central vein areas selected randomly in each specimen.

Confocal Laser-Scanning Microscope

For double staining for OSM and ED2, the sections were incubated with goat anti-mouse OSM antibody and sequentially with horseradish peroxidase-conjugated donkey anti-goat IgG antibody, biotinyl tyramine, and fluorescein isothiocyanate-conjugated streptavidin. After washing, the sections were incubated with mouse anti-rat ED2 antibody (Serotec Ltd., Oxford, UK) and then with R-phycoerythrin-conjugated goat anti-mouse IgG (DAKO) and covered with mounting medium for fluorescence with 4′,6-diamidino-2-phenylindole (Vectashield; Vector Laboratories, Inc., Burlingame, CA). Co-localization of fluorescein isothiocyanate and R-phycoerythrin was analyzed with a confocal laser-scanning microscope (LSM510; Carl Zeiss Jena GmbH, Jena, Germany).

Statistical Analysis

Statistical analysis was performed by unpaired, two-tailed Student's *t*-test. A P value <0.05 was considered significant.

Results

Introduction of HVJ-OSM into the Spleen and Expression of OSM at the Protein Level in the Liver

We injected rat OSM cDNA in HVJ envelope (HVJ-OSM) into the spleens of rats weekly for 3 weeks (Figure 1) and analyzed the liver immunohistochemically. The results showed that OSM protein was exclusively expressed in small cells lining the sinusoid of the liver, whereas OSM-positive cells were hardly detectable in the liver of rats injected with HVJ-Vector (Figure 2, A and B). Because the location of OSM protein-expressing cells appeared to correspond to that of Kupffer cells, we performed immunohistochemical double staining of ED2 and OSM. Kupffer cells identified by ED2 expression were found to be positive for OSM protein (Figure 2, C–E), indicating that injection of OSM cDNA into the spleen resulted in expression at the protein level exclusively in Kupffer cells of the liver.

Repeated Injection of HVJ-OSM Attenuates Liver Damage

First, we examined whether the introduction of OSM cDNA weekly for 3 weeks affects the physiological condition of rats. There is no significant difference between rats injected with HVJ-OSM and with HVJ-Vector in the body weight, liver weight, serum albumin level, and serum liver injury parameters (T-Bil, D-Bil, AST, and ALT values), and a serum fibrosis parameter (hyaluronic acid value), and no obvious liver damage in both these rats (Supplemental Figure S1 available at *http://ajp.amjpathol.org*). Histology of livers showed no significant difference between rats injected with HVJ-OSM and with HVJ-Vector (Supplemental Figure S2 available at *http://ajp.amjpathol.org*). These results indicated that the introduction of OSM cDNA does not affect the physiological conditions of rats.

Next, we examined the effect of OSM cDNA introduction on rats damaged by DMN. Rats injected with HVJ-OSM and HVJ-Vector weighed 164 ± 6 and 149 ± 3 g, respectively, indicating that the OSM introduction leads to the improvement of the general condition of DMN-damaged rats (Figure 3). We then analyzed the pathological state of livers by examining the liver weight, serum albumin levels, and serum liver injury parameters, ie, T-Bil, D-Bil, AST, and ALT values. Liver weights and serum albumin values of rats injected with HVJ-OSM were significantly higher than those of rats injected with HVJ-Vector, and all serum liver injury parameters were significantly lower (Figure 3). We also analyzed a serum fibrosis parameter, hyaluronic acid value, and found that hyaluronic acid value of rats injected with HVJ-OSM was significantly lower than that of rats injected with HVJ-Vector (Figure 3). These results showed that the fibrogenesis of rats injected with HVJ-OSM was less than those injected with HVJ-Vector. In addition, we examined histology of the liver. In the liver of rats injected with HVJ-Vector, centrilobular necrosis and numerous inflammatory cells were observed (Figure 4A). On the other hand, rats injected with HVJ-OSM showed much less centrilobular necrosis and a smaller number of inflammatory cells (Figure 4B). The development of liver fibrosis was inhibited by HVJ-OSM injection (Figure 4, C and D). Taken together, these results indicate that the repeated injection of HVJ-OSM attenuates DMN-induced liver damage and stimulates regeneration.

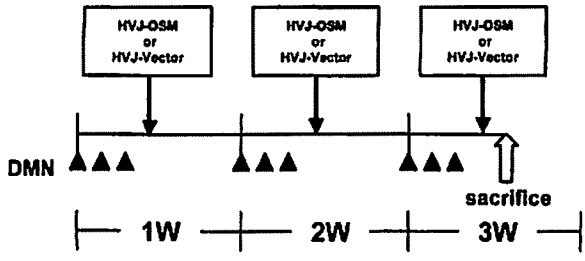

Figure 1. Schedule of DMN administration and HVJ-OSM or HVJ-Vector injection. Rats were given DMN intraperitoneally at 15 mg/kg body weight for 3 consecutive days per week for 3 weeks. On day 4 of each week, HVJ-OSM or HVJ-Vector was injected into the spleen. On day 5 of the last week, rats were sacrificed for analysis. w, week

Effects of HVJ-OSM Transfection on Proliferation and Apoptosis of Hepatocytes

To evaluate the effects of HVJ-OSM injection on proliferative activity of hepatocytes, we examined the density of hepatocytes and the percentage of hepatocytes expressing Ki-67. Histological examination showed that rats injected with HVJ-OSM contained a much larger number of hepatocytes around the portal field than those injected with HVJ-Vector (Figure 5, A, B, and G). Immunohistochemical examination of Ki-67 showed that Ki-67-expressing cells were mainly hepatocytes in rats injected with HVJ-OSM, whereas they were inflammation cells in rats injected with HVJ-Vector (Figure 5, C and D). The proportion of Ki-67-positive hepatocytes to total hepatocytes in portal field was significantly higher in rats injected with HVJ-OSM than those injected with HVJ-Vector (Figure 5H). These results indicate that repeated injection of HVJ-OSM augments hepatocyte proliferation.

Because DMN is known to induce apoptosis as well as necrosis of hepatocytes,[24,25] we examined whether repeated injection of HVJ-OSM prevents apoptosis of hepatocytes. The proportion of TUNEL-positive hepatocytes to total hepatocytes in central vein area (0.25 mm^2) of HVJ-OSM-injected livers was 0.4 ± 0.1, which was much less than that of HVJ-Vector-injected livers, 2.2 ± 0.2 (Figure 5, E, F, and I). These results indicate that

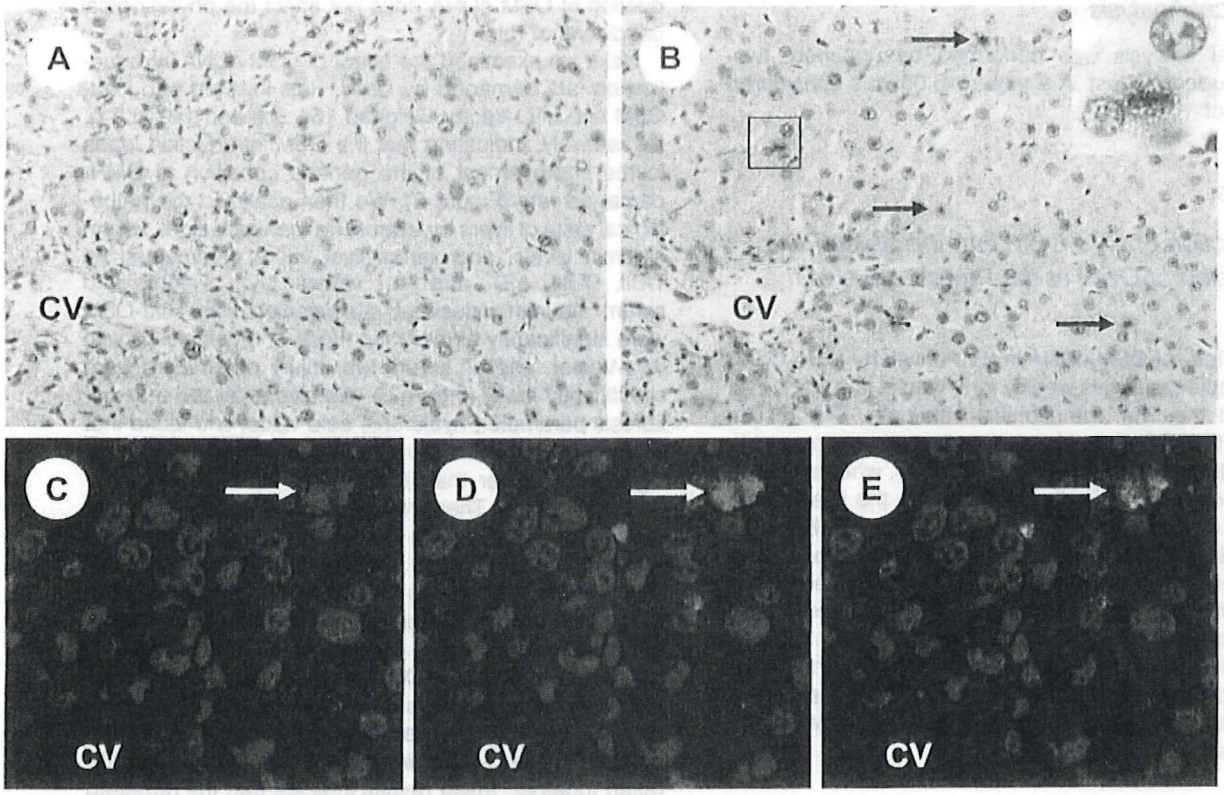

Figure 2. Expression of OSM in the liver of a rat injected with HVJ-OSM. **A:** Immunostaining of OSM in the liver of a rat injected with HVJ-Vector. **B:** Immunostaining of OSM in the liver of a rat injected with HVJ-OSM. **Arrows** indicate representative OSM-expressing cells. **Inset** in **B** is a higher magnification of the squared region, and shows an OSM-expressing cell. **C:** Fluorescein for ED2, which is a marker of Kupffer cells (red). **D:** Fluorescein for OSM (green). **E:** Merged confocal image of **C** and **D**. Coexpression of ED2 and OSM is shown as yellow. **White arrows** indicate representative coexpression of ED2 and OSM. **C** to **E** are photographs of the same section, taken by confocal laser-scanning microscope. CV, central vein. Original magnifications: ×200 (**A** and **B**); ×600 (**inset**).

repeated injection of HVJ-OSM prevents apoptosis of hepatocytes.

Time-Course Studies on osm Gene Therapy before or after DMN Treatment

To clarify the biological role of OSM on livers damaged by DMN, we performed time-course studies of the effect of OSM cDNA introduction before or after DMN treatment. In the case of OSM pretreatment, AST and ALT values of rats injected with HVJ-OSM were lower than those of rats injected with HVJ-Vector on days 1 and 2 after DMN treatment. T-Bil and D-Bil values of rats injected with HVJ-OSM were also lower than those of rats injected with HVJ-Vector on day 2 (Figure 6). Centrilobular necrosis caused by subsequent treatment with DMN was much less in rats pretreated with HVJ-OSM than those pretreated with HVJ-Vector (Figure 7). These results indicate that OSM protects livers from cytotoxicity caused by DMN. In the case of posttreatment, serum liver injury parameters (AST, ALT, T-Bil, and D-Bil values) were improved in rats injected with HVJ-OSM, as compared with those injected with HVJ-Vector, on day 1 after HVJ-OSM introduction (Figure 6). Histological study showed that centrilobular necrosis induced by DMN disappeared more rapidly in rats injected with HVJ-OSM than in rats injected with HVJ-Vector (Figure 8). These results indicate that OSM promotes liver regeneration. Thus, OSM is able to protect livers from cytotoxicity caused by DMN and also accelerate regeneration of liver damaged by DMN.

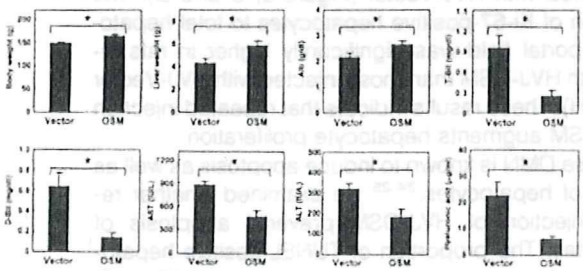

Figure 3. Effects of OSM on body weight, liver weight, serum albumin levels, serum liver injury parameters, and serum, a fibrosis parameter in rats with DMN-induced liver damage. Vector: Rats injected with HVJ-Vector. OSM: Rats injected with HVJ-OSM. Alb, albumin. Data represent the mean of six rats. Bars are standard errors. $^{*}P < 0.05$, significant difference by *t*-tests.

Discussion

OSM was originally characterized by its ability to inhibit the proliferation of tumor cells,[17,18,26] but since then it has been shown to be involved in inflammation, hemato-

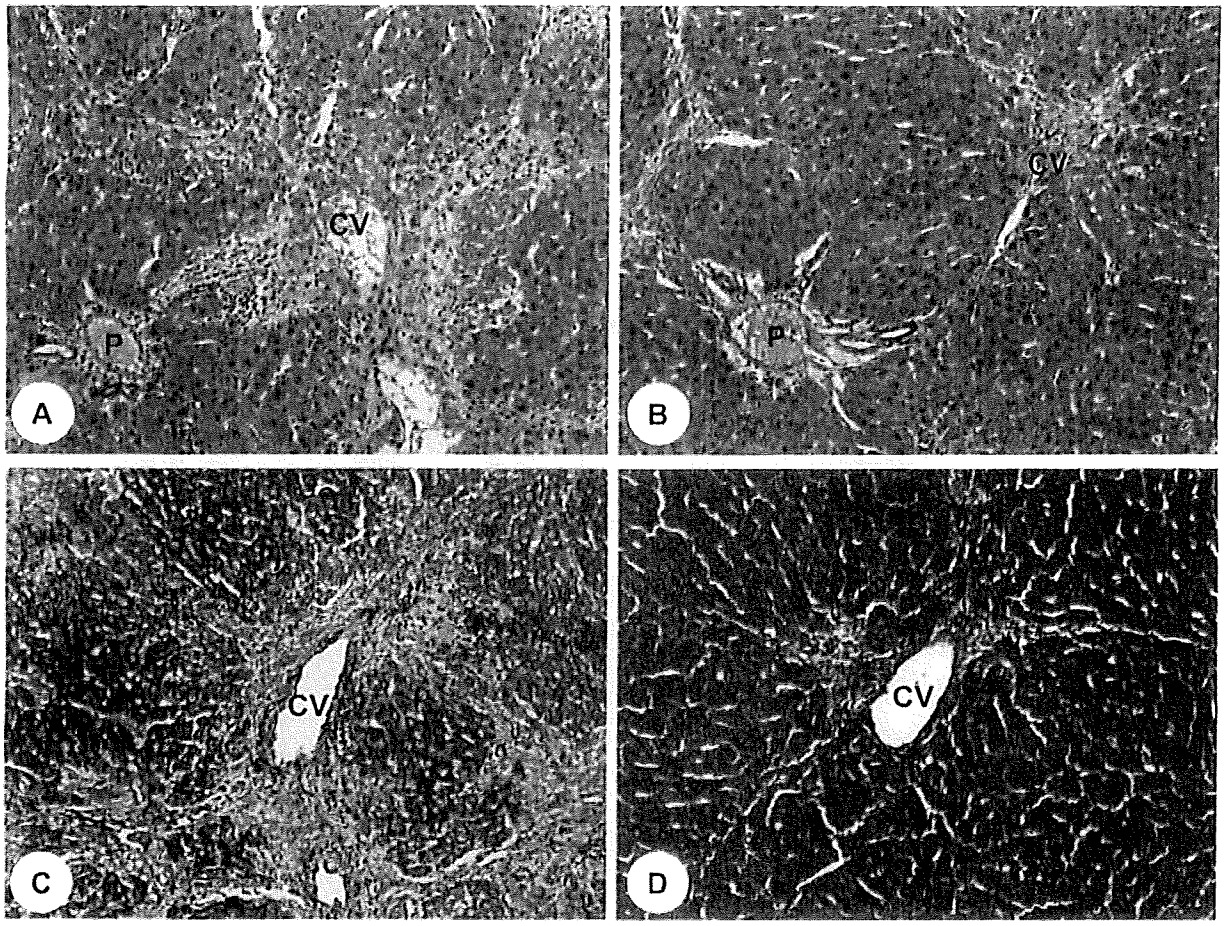

Figure 4. Histology of livers of rats injected with HVJ-Vector or HVJ-OSM. **A** and **C**: Liver sections of a rat injected with HVJ-Vector. **B** and **D**: Liver sections of a rat injected with HVJ-OSM. Sections of **A** and **B** were stained with H&E, and those of **C** and **D** with Azan. P, portal vein; CV, central vein. Original magnifications ×90 (**A** and **B**); ×100 (**C** and **D**).

poiesis, embryonic development, and tissue remodeling.[17,18,27] In addition, OSM has recently been shown to play an important role in liver development and regeneration.[17,18,20–22,28] In this study, we examined whether the introduction of rat OSM cDNA enhances the regeneration of rat livers damaged by DMN. Repeated injection of HVJ-OSM into the spleen resulted in increases in body weight, liver weight, and serum albumin levels and the reduction of serum parameters of liver injury and fibrosis. Moreover, histologically, *osm* gene therapy reduced centrilobular necrosis and inflammatory cell infiltration, promoted hepatocyte proliferation, and suppressed hepatocyte apoptosis. The fibrosis identified by Azan stain was also attenuated by *osm* gene therapy. These results indicate that OSM is a key mediator for proliferation and anti-apoptosis of hepatocytes and suggest that *osm* gene therapy is useful for the treatment of patients with liver damage.

Time-course studies on the effect of HVJ-OSM treatment on subsequent liver injury caused by DMN showed that serum liver injury parameters (T-Bil, D-Bil, AST, and ALT values) of rats pretreated with HVJ-OSM were lower than those of rats pretreated with HVJ-Vector. Centrilobular necrosis caused by subsequent treatment with DMN was also much less in rats pretreated with HVJ-OSM than those pretreated with HVJ-Vector. Time-course studies on HVJ-OSM treatment after DMN injury showed that serum AST, ALT, T-Bil, and D-Bil values were improved in rats injected with HVJ-OSM after HVJ-OSM introduction. Centrilobular necrosis induced by DMN was also shown to disappear more rapidly in rats injected with HVJ-OSM than in rats injected with HVJ-Vector. These results indicate that OSM is effective in combating DMN-caused liver injury by administrating either before or after DMN treatment, suggest that *osm* gene therapy is useful, as preventive and curative means, for the treatment of liver injury.

In this study, we directly injected HVJ-OSM into the spleen of rats with DMN-damaged livers. HVJ-OSM injected into the spleen is expected to reach the liver, because the blood of spleen flows into the portal vein through the splenic hilus. The HVJ envelope is ~280 nm in diameter,[23] whereas the diameter of the fenestrae of sinusoidal endothelial cells, which separate sinusoidal blood from the space of Disse, is ~175 nm in the periportal area,[29] indicating that HVJ-OSM hardly go through

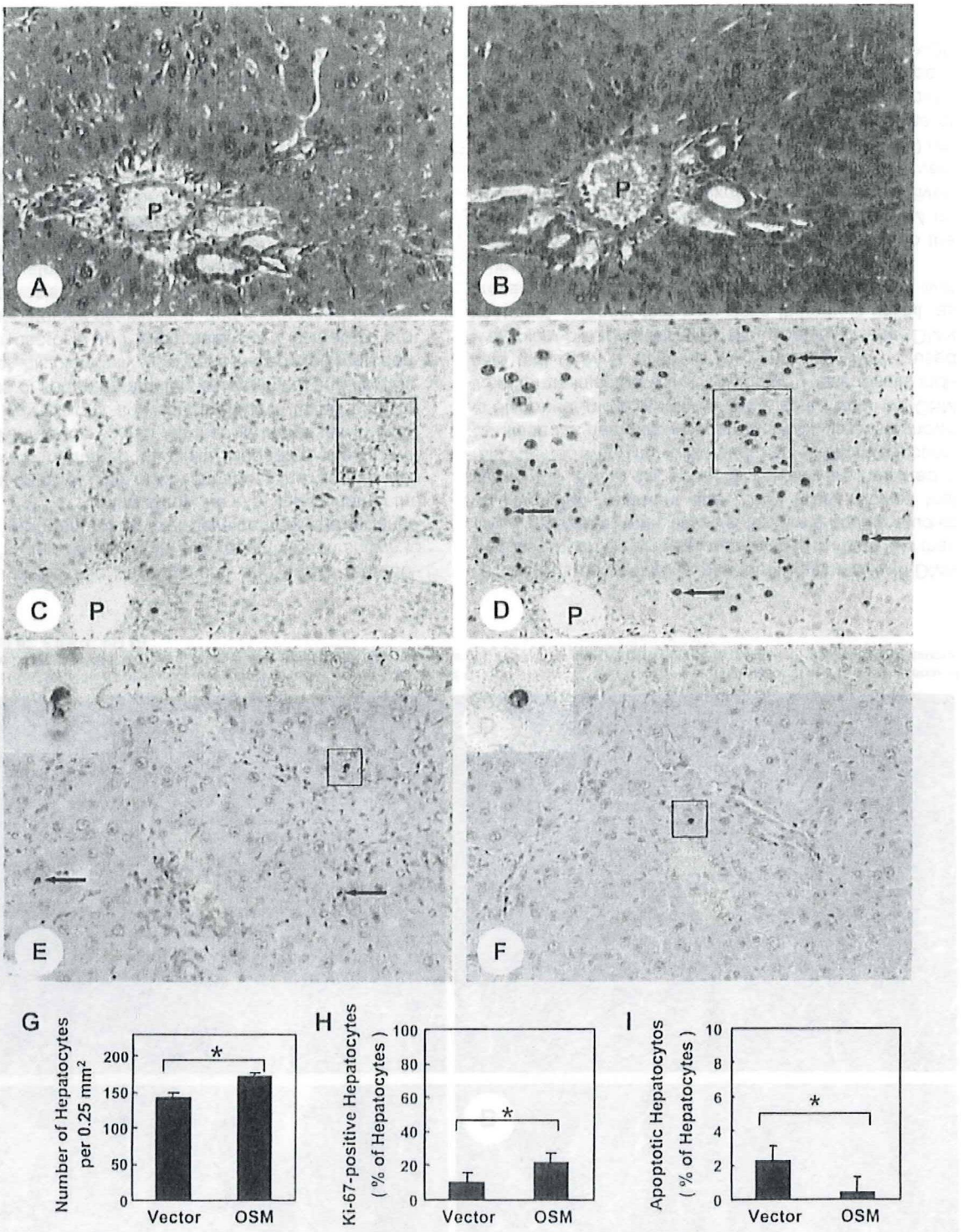

Figure 5. Effects of OSM on proliferation and apoptosis of hepatocytes in rats with DMN-induced liver damage. **A**, **C**, and **E**: Liver sections of a rat injected with HVJ-Vector. **B**, **D**, and **F**: Liver sections of a rat injected with HVJ-OSM. Sections of **A** and **B** were stained with H&E, those of **C** and **D** were immunostained with Ki-67 antibody, and those of **E** and **F** were subjected to TUNEL staining. **Arrows** in **D** and **E** indicate representative Ki-67-positive and apoptotic hepatocytes, respectively. The **inset** in **C** is a high magnification of the squared region and shows inflammatory cells expressing Ki-67 antigen. The **inset** in **D** is a high magnification of the squared region and shows hepatocytes expressing Ki-67 antigen. Each **inset** in **E** and **F** is a high magnification of the squared region and shows apoptotic hepatocytes. P, portal vein. **G** and **H** show the number of total hepatocytes per portal field and the proportion of Ki-67-positive hepatocytes to total hepatocytes, respectively. **I** shows the proportion of TUNEL-positive hepatocytes to total hepatocytes. Data represent the mean of six rats. Bars are standard errors. $^*P < 0.05$, significant difference by *t*-tests. Vector: Rats injected with HVJ-Vector. OSM: Rats injected with HVJ-OSM. Original magnifications: ×150 (**A** and **B**); ×100 (**C** and **D**); ×170 (**E** and **F**); ×160 (**C** and **D**, **insets**); ×520 (**E** and **F**, **insets**).

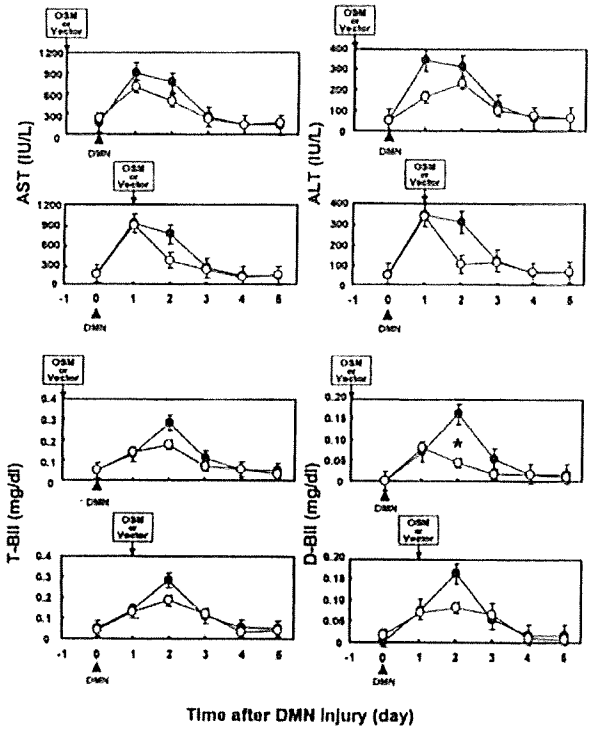

Figure 6. Time-course studies of the effect of OSM treatment before or after DMN injury on serum liver injury parameters in rats with DMN-induced liver damage (●). Rats injected with HVJ-Vector. (○). Rats injected with HVJ-OSM. Data represent the mean of three rats. Bars are standard errors. *$P < 0.05$, significant difference by *t*-tests

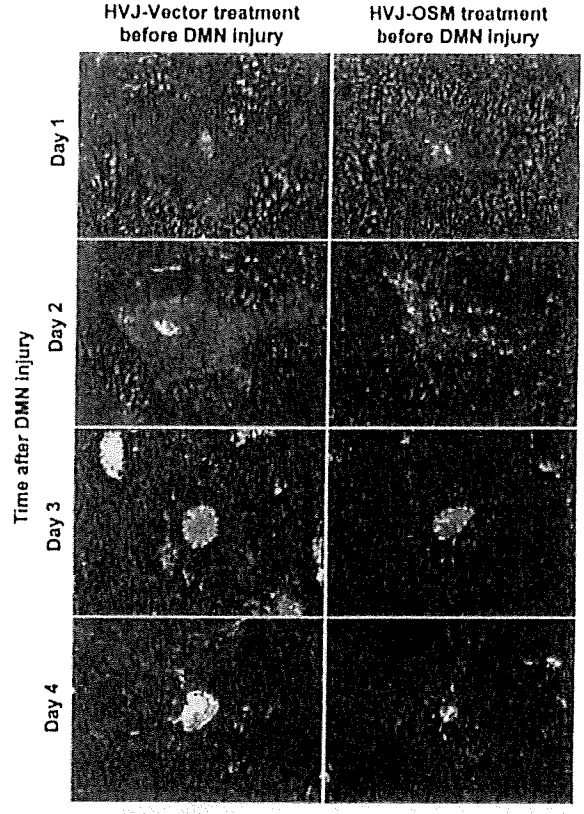

Figure 7. Time-course studies on the liver histology of rats injected with HVJ-Vector or HVJ-OSM before DMN injury. Sections were stained with H&E. Original magnifications, ×40

the fenestrae of sinusoidal endothelial cells. It is, therefore, likely that HVJ-OSM may be retained in Kupffer cells, which are present within the sinusoid. Ogushi and colleagues[30] reported that when mice were injected with fluorescein isothiocyanate-labeled oligodeoxynucleotides encapsulated HVJ liposome into the spleen, more than 95% of fluorescein isothiocyanate-labeled oligodeoxynucleotides were transferred into Kupffer cells and only 1% into endothelial cells of the liver. These findings supported the present results that OSM protein was found exclusively in Kupffer cells after injection of OSM cDNA into the spleen.

The role of OSM in inflammatory responses is complex, performing in either a proinflammatory or an anti-inflammatory manner. In proinflammatory action, OSM increases P-selectin expression, induces granulocyte-macrophage colony-stimulating factor (GM-CSF), granulocyte colony-stimulating factor, and IL-6 secretion in endothelial cells *in vitro*, and causes an inflammatory response when injected subcutaneously into mice.[31–34] On the other hand, in anti-inflammatory action, OSM induces tissue inhibitor of metalloproteinase-1 (TIMP-1)[35] and down-regulates IL-1-induced proinflammatory mediators, such as IL-8, GM-CSF, and RANTES, in human fibroblasts.[36] Transfection of mouse *osm* gene in adenoviral vector has also been shown to induce acute-phase proteins and TIMP-1 expression in mice.[37] The present study showed that repeated injection of HVJ-OSM into the spleen of rats with DMN-induced liver damage significantly reduced centrilobular necrosis and the infiltration of inflammatory cells into the damaged sites of livers. Consistent with these findings, Sanchez and colleagues[38] have reported that adenoviral transfer of *osm* gene suppresses dextran-sodium sulfate-induced colitis in mice by reducing macrophage infiltration and apoptosis. These results support the role of OSM as an anti-inflammatory cytokine.

Recently, OSM-R$^{-/-}$ mice have been shown to decrease in proliferating cell nuclear antigen-positive hepatocytes after CCl_4-induced liver damage.[21] It has also been shown that restoration of liver mass after 70% hepatectomy is delayed in OSM-R$^{-/-}$ mice.[21] In this study, we found that the number of total hepatocytes and the proportion of Ki-67-positive hepatocytes to total hepatocytes of rats injected with HVJ-OSM were significantly higher than those injected with HVJ-Vector. These results suggest that OSM-R-mediated signaling is required for the proliferative response of hepatocytes in damaged liver. In human adipose tissue-derived mesenchymal stem cells, two separate signaling pathways, MEK/ERK and JAK3/STAT1, have been shown to be independently involved in the OSM-stimulated proliferation.[39] It is therefore possible that these two separate signaling pathways participate in OSM-stimulated proliferation of hepatocytes in the liver regeneration, resulting in a striking hepatocyte growth. Recently, Cohen and colleagues[40] reported a specific up-regulation of HGF synthesis by OSM, most likely through the MAPK pathway, in human

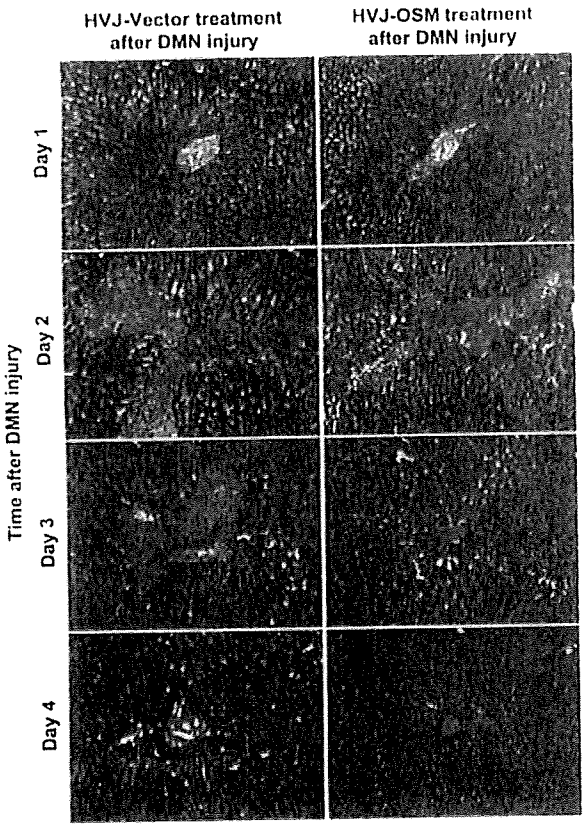

Figure 8. Time-course studies on the liver histology of rats injected with HVJ-Vector or HVJ-OSM after DMN injury. Sections were stained with H&E. Original magnifications, ×40.

lung fibroblasts, suggesting that OSM participates in lung repair through HGF production. Because HGF is an important growth factor for hepatocytes, the up-regulation of HGF synthesis by OSM may be involved in the proliferation of hepatocytes in the liver regeneration. The AP-1 transcription factor c-Jun is a key regulator of hepatocyte proliferation. Mice lacking c-Jun display impaired liver regeneration after partial hepatectomy. Liver regeneration is regulated by c-Jun/AP-1 through a pathway involving p53, p21, and the stress kinase p38α.[41] These molecules may be also involved in OSM-stimulated liver regeneration. However, the mechanism by which OSM prevents liver injury and enhances liver regeneration remains to be clarified.

In addition, we found that *osm* gene therapy reduced apoptosis of hepatocytes. A number of studies have shown that STAT3 activated by IL-6 exhibits anti-apoptotic effects through the induction of Bcl-2, Bcl-xL, and FLICE inhibitor protein, which in turn inhibits FLICE and caspase-3 in hepatocytes.[42,43] Adenovirus-mediated expression of an active form of STAT3 has also been shown to induce the expression of redox-associated protein redox factor-1 and reduce Fas-mediated apoptosis in the liver.[44] Because OSM is known to activate STAT3,[17,18] it is possible that OSM may reduce DMN-induced apoptosis of hepatocytes through STAT3 activation.

DMN induces liver fibrosis in a highly reproducible manner, first inducing a central hemorrhagic necrosis followed by the formation of septa and establishing micronodular cirrhosis after 3 weeks of treatment.[45] Biological and ultrastructural studies suggest that inflammatory mechanisms are involved in DMN-induced liver fibrosis.[45–48] The present study showed that *osm* gene therapy could suppress liver fibrosis induced by DMN. Because OSM may function as an anti-inflammatory cytokine, as mentioned above, there is a possibility that the production of inflammatory cytokines involved in fibrosis is suppressed by *osm* gene therapy. Alternatively, the tissue repair by fibrosis is not indispensable because OSM induces the proliferation of hepatocytes to fill the space of centrilobular necrosis caused by DMN.

The response to partial hepatectomy is impaired in IL-6-deficient mice.[6] The studies using liver-specific conditional knockout mice have also shown that activation of STAT3 is required for liver regeneration.[49] These findings demonstrate that IL-6 and a downstream mediator of IL-6 signaling pathway, STAT3, are very important molecules for liver regeneration. OSM, like IL-6, activates Jak1, Jak2, and Tyk2 and the activated Jaks in turn activate STAT3.[17,18] Recently, Nakamura and colleagues[21] have shown that liver regeneration is impaired in OSM-R$^{-/-}$ mice as well as IL-6$^{-/-}$ mice. They have also shown that OSM expression after CCl_4 exposure is greatly decreased in IL-6$^{-/-}$ mice, whereas IL-6 expression after CCl_4 exposure is not altered in OSMR$^{-/-}$ mice. Moreover, OSM administration in IL-6$^{-/-}$ mice has been shown to induce phosphorylation of STAT3 with the normal kinetics. These results suggest that OSM is a downstream mediator of IL-6 in liver regeneration. Therefore, it is likely that *osm* gene therapy may be more direct and efficient than the therapy using *il-6* gene in the treatment of patients with liver damage.

OSM-R is hardly expressed in hepatocytes in mouse and human livers.[21,50] This may reflect very low levels of proliferation of hepatocytes in normal liver. On the other hand, the expression of OSM-R has been shown to rapidly increase in hepatocytes after liver injury.[21] Therefore, it is proposed that, in *osm* gene therapy, a large number of OSM-R in injured hepatocytes interacts with OSM generated from the introduced gene to inhibit hepatocyte apoptosis and promote hepatocyte proliferation, leading to active liver regeneration.

Acknowledgments

We thank Ms. Michiko Kakihana, Ms. Mio Kawasumi, and Mr. Hirotsugu Kubo, Hyogo College of Medicine, for their technical assistance.

References

1. Fausto N, Laird AD, Webber EM. Liver regeneration. 2. Role of growth factors and cytokines in hepatic regeneration. FASEB J. 1995; 9:1527–1536
2. Michalopoulos GK, DeFrances MC. Liver regeneration. Science. 1997; 276:60–66

3. Lindroos PM, Zarnegar R, Michalopoulos GK: Hepatocyte growth factor (hepatopoietin A) rapidly increases in plasma before DNA synthesis and liver regeneration stimulated by partial hepatectomy and carbon tetrachloride administration. Hepatology 1991, 13: 743–750
4. Rubin RA, O'Keefe EJ, Earp HS: Alteration of epidermal growth factor-dependent phosphorylation during rat liver regeneration. Proc Natl Acad Sci USA 1982, 79:776–780
5. Webber EM, FitzGerald MJ, Brown PI, Bartlett MH, Fausto N: Transforming growth factor-alpha expression during liver regeneration after partial hepatectomy and toxic injury, and potential interactions between transforming growth factor-alpha and hepatocyte growth factor. Hepatology 1993, 18:1422–1431
6. Yamada Y, Fausto N: Deficient liver regeneration after carbon tetrachloride injury in mice lacking type 1 but not type 2 tumor necrosis factor receptor. Am J Pathol 1998, 152:1577–1589
7. Webber EM, Bruix J, Pierce RH, Fausto N: Tumor necrosis factor primes hepatocytes for DNA replication in the rat. Hepatology 1998, 28:1226–1234
8. Cressman DE, Greenbaum LE, DeAngelis RA, Ciliberto G, Furth EE, Poli V, Taub R: Liver failure and defective hepatocyte regeneration in interleukin-6-deficient mice. Science 1996, 274:1379–1383
9. Kovalovich K, DeAngelis RA, Li W, Furth EE, Ciliberto G, Taub R: Increased toxin-induced liver injury and fibrosis in interleukin-6-deficient mice. Hepatology 2000, 31:149–159
10. Gohda E, Tsubouchi H, Nakayama H, Hirono S, Sakiyama O, Takahashi K, Miyazaki H, Hashimoto S, Daikuhara Y: Purification and partial characterization of hepatocyte growth factor from plasma of a patient with fulminant hepatic failure. J Clin Invest 1988, 81:414–419
11. Okano J, Shiota G, Kawasaki H: Protective action of hepatocyte growth factor for acute liver injury caused by D-galactosamine in transgenic mice. Hepatology 1997, 26:1241–1249
12. Kosai K, Matsumoto K, Funakoshi H, Nakamura T: Hepatocyte growth factor prevents endotoxin-induced lethal hepatic failure in mice. Hepatology 1999, 30:151–159
13. Matsuda Y, Matsumoto K, Yamada A, Ichida T, Asakura H, Komoriya Y, Nishiyama E, Nakamura T: Preventive and therapeutic effects in rats of hepatocyte growth factor infusion on liver fibrosis/cirrhosis. Hepatology 1997, 26:81–89
14. Ueki T, Kaneda Y, Tsutsui H, Nakanishi K, Sawa Y, Morishita R, Matsumoto K, Nakamura T, Takahashi H, Okamoto E, Fujimoto J: Hepatocyte growth factor gene therapy of liver cirrhosis in rats. Nat Med 1999, 5:226–230
15. Gómez-Lechón MJ: Oncostatin M: signal transduction and biological activity. Life Sci 1999, 65:2019–2030
16. Taga T, Kishimoto T: Gp130 and the interleukin-6 family of cytokines. Annu Rev Immunol 1997, 15:797–819
17. Miyajima A, Kinoshita T, Tanaka M, Kamiya A, Mukouyama Y, Hara T: Role of Oncostatin M in hematopoiesis and liver development. Cytokine Growth Factor Rev 2000, 11:177–183
18. Tanaka M, Miyajima A: Oncostatin M, a multifunctional cytokine. Rev Physiol Biochem Pharmacol 2003, 149:39–52
19. Tanaka M, Hara T, Copeland NG, Gilbert DJ, Jenkins NA, Miyajima A: Reconstitution of the functional mouse oncostatin M (OSM) receptor: molecular cloning of the mouse OSM receptor β subunit. Blood 1999, 93:804–815
20. Kamiya A, Kinoshita T, Ito Y, Matsui T, Morikawa Y, Senba E, Nakashima K, Taga T, Yoshida K, Kishimoto T, Miyajima A: Fetal liver development requires a paracrine action of oncostatin M through the gp130 signal transducer. EMBO J 1999, 18:2127–2136
21. Nakamura K, Nonaka H, Saito H, Tanaka M, Miyajima A: Hepatocyte proliferation and tissue remodeling is impaired after liver injury in oncostatin M receptor knockout mice. Hepatology 2004, 39:635–644
22. Okaya A, Kitanaka J, Kitanaka N, Satake M, Kim Y, Terada K, Sugiyama T, Takemura M, Fujimoto J, Terada N, Miyajima A, Tsujimura T: Oncostatin M inhibits proliferation of rat oval cells, OC15-5, inducing differentiation into hepatocytes. Am J Pathol 2005, 166:709–719
23. Kaneda Y, Tabata Y: Non-viral vectors for cancer therapy. Cancer Sci 2006, 97:348–354
24. Pritchard DJ, Butler WH: Apoptosis—the mechanism of cell death in dimethylnitrosamine-induced hepatotoxicity. J Pathol 1989, 158: 253–260
25. Horn TL, Bhattacharjee A, Schook LB, Rutherford MS: Altered hepatic mRNA expression of apoptotic genes during dimethylnitrosamine exposure. Toxicol Sci 2000, 57:240–249
26. Zarling JM, Shoyab M, Marquardt H, Hanson MB, Lioubin MN, Todaro GJ: Oncostatin M: a growth regulator produced by differentiated histiocytic lymphoma cells. Proc Natl Acad Sci USA 1986, 83: 9739–9743
27. Wallace PM, MacMaster JF, Rouleau KA, Brown TJ, Loy JK, Donaldson KL, Wahl AF: Regulation of inflammatory responses by oncostatin M. J Immunol 1999, 162:5547–5555
28. Kinoshita T, Sekiguchi T, Xu MJ, Ito Y, Kamiya A, Tsuji K, Nakahata T, Miyajima A: Hepatic differentiation induced by oncostatin M attenuates fetal liver hematopoiesis. Proc Natl Acad Sci USA 1999, 96:7265–7270
29. Wisse E, De Zanger RB, Charels K, Van Der Smissen P, McCuskey RS: The liver sieve: considerations concerning the structure and function of endothelial fenestrae, the sinusoidal wall and the space of Disse. Hepatology 1985, 5:683–692
30. Ogushi I, Iimuro Y, Seki E, Son G, Hirano T, Hada T, Tsutsui H, Nakanishi K, Morishita R, Kaneda Y, Fujimoto J: Nuclear factor κB decoy oligodeoxynucleotides prevent endotoxin-induced fetal liver failure in a murine model. Hepatology 2003, 38:335–344
31. Brown TJ, Liu J, Brashem-Stein C, Shoyab M: Regulation of granulocyte colony-stimulating factor and granulocyte-macrophage colony-stimulating factor expression by oncostatin M. Blood 1993, 82:33–37
32. Brown TJ, Rowe JM, Liu JW, Shoyab M: Regulation of IL-6 expression by oncostatin M. J Immunol 1991, 147:2175–2180
33. Yao L, Pan J, Setiadi H, Patel KD, McEver RP: Interleukin 4 or oncostatin M induces a prolonged increase in P-selectin mRNA and protein in human endothelial cells. J Exp Med 1996, 184:81–92
34. Modur V, Feldhaus MJ, Weyrich AS, Jicha DL, Prescott SM, Zimmerman GA, McIntyre TM: Oncostatin M is a proinflammatory mediator. In vivo effects correlate with endothelial cell expression of inflammatory cytokines and adhesion molecules. J Clin Invest 1997, 100:158–168
35. Richards CD, Shoyab M, Brown TJ, Gauldie J: Selective regulation of metalloproteinase inhibitor (TIMP-1) by oncostatin M in fibroblasts in culture. J Immunol 1993, 150:5596–5603
36. Richards CD, Langdon C, Botelho F, Brown TJ, Agro A: Oncostatin M inhibits IL-1-induced expression of IL-8 and granulocyte-macrophage colony-stimulating factor by synovial and lung fibroblasts. J Immunol 1996, 156:343–349
37. Kerr C, Langdon C, Graham F, Gauldie J, Hara T, Richards CD: Adenovirus vector expressing mouse oncostatin M induces acute-phase proteins and TIMP-1 expression in vivo in mice. J Interferon Cytokine Res 1999, 19:1195–1205
38. Sanchez AL, Langdon CM, Akhtar M, Lu J, Richards CD, Bercik P, McKay DM: Adenoviral transfer of the murine oncostatin M gene suppresses dextran-sodium sulfate-induced colitis. J Interferon Cytokine Res 2003, 23:193–201
39. Song HY, Jeon ES, Jung JS, Kim JH: Oncostatin M induces proliferation of human adipose tissue-derived mesenchymal stem cells. Int J Biochem Cell Biol 2005, 37:2357–2365
40. Cohen M, Marchand-Adam S, Lecon-Malas V, Marchal-Somme J, Boutten A, Durand G, Crestani B, Dehoux M: HGF synthesis in human lung fibroblasts is regulated by oncostatin M. Am J Physiol 2006, 290:L1097–L1103
41. Stepniak E, Ricci R, Eferl R, Sumara G, Sumara I, Rath M, Hui L, Wagner EF: c-Jun/AP-1 controls liver regeneration by repressing p53/p21 and p38 MAPK activity. Genes Dev 2006, 20:2306–2314
42. Fukada T, Hibi M, Yamanaka Y, Takahashi-Tezuka M, Fujitani Y, Yamaguchi T, Nakajima K, Hirano T: Two signals are necessary for cell proliferation induced by a cytokine receptor gp130: involvement of STAT3 in anti-apoptosis. Immunity 1996, 5:449–460
43. Kovalovich K, Li W, DeAngelis R, Greenbaum LE, Ciliberto G, Taub R: Interleukin-6 protects against Fas-mediated death by establishing a critical level of anti-apoptotic hepatic proteins FLIP, Bcl-2, and Bcl-xL. J Biol Chem 2001, 276:26605–26613
44. Haga S, Terui K, Zhang HQ, Enosawa S, Ogawa W, Inoue H, Okuyama T, Takeda K, Akira S, Ogino T, Irani K, Ozaki M: Stat3 protects against Fas-induced liver injury by redox-dependent and -independent mechanisms. J Clin Invest 2003, 112:989–998
45. Jézéquel AM, Mancini R, Rinaldesi ML, Macarri G, Venturini C, Orlandi F: A morphological study of the early stages of hepatic

fibrosis induced by low doses of dimethylnitrosamine in the rat. J Hepatol 1987, 5:174–181
46. Jézéquel AM, Mancini R, Rinaldesi ML, Ballardini G, Fallani M, Bianchi F, Orlandi F: Dimethylnitrosamine-induced cirrhosis. Evidence for an immunological mechanism. J Hepatol 1989, 8:42–52
47. Myers MJ, Schook LB: Immunotoxicity of nitrosamines. Experimental Immunotoxicology. Edited by RJ Smialowicz, MP Holsapple. Boca Raton, CRC Press, 1996, pp 351–366
48. Jin YL, Enzan H, Kuroda N, Hayashi Y, Toi M, Miyazaki E, Hamauzu T, Hiroi M, Guo LM, Shen ZS, Saibara T: Vascularization in tissue remodeling after rat hepatic necrosis induced by dimethylnitrosamine. Med Mol Morphol 2006, 39:33–43
49. Li W, Liang X, Kellendonk C, Poli V, Taub R: STAT3 contributes to the mitogenic response of hepatocytes during liver regeneration. J Biol Chem 2002, 277:28411–28417
50. Znoyko I, Sohara N, Spicer SS, Trojanowska M, Reuben A: Expression of oncostatin M and its receptors in normal and cirrhotic human liver. J Hepatol 2005, 43:893–900

Liver International ISSN 1478-3223

CLINICAL STUDIES

Differences in molecular alterations of hepatocellular carcinoma between patients with a sustained virological response and those with hepatitis C virus infection

Takehiro Hayashi[1,2], Akihiro Tamori[1], Manabu Nishikawa[3], Hiroyasu Morikawa[1], Masaru Enomoto[1], Hiroki Sakaguchi[1], Daiki Habu[1], Norifumi Kawada[1], Shoji Kubo[4], Shuhei Nishiguchi[5] and Susumu Shiomi[2]

1 Department of Hepatology, Osaka City University Graduate School of Medicine, Osaka, Japan
2 Department of Nuclear Medicine, Osaka City University Graduate School of Medicine, Osaka, Japan
3 Department of Biochemistry and Molecular Pathology, Osaka City University Graduate School of Medicine, Osaka, Japan
4 Department of Surgery, Osaka City University Graduate School of Medicine, Osaka, Japan
5 Department of Internal Medicine, Hyogo College of Medicine, Nishinomiya, Japan

Keywords
hepatitis C virus – hepatocellular carcinoma – hypermethylation – interferon – mitochondrial DNA – *p16* – *p53* – sustained virological response

Correspondence
Akihiro Tamori, MD, Department of Hepatology, Osaka City University Graduate School of Medicine, 1-4-3 Asahimachi, Abeno-ku, Osaka 545-8585, Japan
Tel: +81 6 6645 2292
Fax: +81 6 6645 1433
e-mail: atamori@med.osaka-cu.ac.jp

Received 16 January 2008
Accepted 16 March 2008

DOI:10.1111/j.1478-3231.2008.01772.x

Abstract

Background/Aims: The mechanism of hepatocarcinogenesis remains unclear in patients in whom hepatitis C virus (HCV) disappears after interferon (IFN) therapy. We compared molecular alterations in hepatocellular carcinoma (HCC) between patients with a sustained virological response (SVR) to IFN and patients with HCV. *Methods:* The study group comprised 44 patients with HCV and 13 patients with SVR. One patient in the SVR group had two tumour nodules, both of which were examined. Mitochondrial DNA (mtDNA) mutations in displacement-loop lesions were directly sequenced. Mutation of the TP53 gene was examined by direct sequencing. The methylation status of *p16*, *p15*, *p14*, *RB* and *PTEN* genes was evaluated by a methylation-specific polymerase chain reaction. *Results:* The average number of mtDNA mutations was 4.2 in 44 HCCs with HCV and 2.0 in 14 HCCs with SVR ($P = 0.0021$). mtDNA mutation was less frequently detected in HCCs from patients with SVR than in patients with HCV. TP53 mutations were detected in 12 (27%) of 44 HCCs with HCV and 2 (14%) of 14 SVR-HCCs. Hypermethylation of the *p16*, *p15*, *p14*, *RB* and *PTEN* promoters was, respectively, detected in 34, 13, 8, 12 and 11 of 44 HCCs from patients with HCV and 14, 0, 0, 2 and 2 of 14 HCCs from patients with SVR ($P = 0.049$, 0.021, 0.085, 0.322 and 0.402). Hypermethylation of *p16* was one of the most important alterations in SVR-HCC. *Conclusions:* Molecular alterations in hepatocarcinogenesis of patients with SVR-HCC were different from those of patients with continuous HCV infection.

Hepatitis C virus (HCV) is one of the most important risk factors for hepatocellular carcinoma (HCC). Clinical studies have suggested that HCV induces inflammation in the liver, followed by the accumulation of reactive oxygen species (ROS), which promote mutations in the human genome (1, 2). Persistent inflammation also results in repeated hepatocyte death and regeneration, leading to the gradual accumulation of DNA mutations in hepatocytes. Point mutations in tumour suppressor genes, including TP53, have been confirmed in hepatic cirrhosis in patients with HCV (3). Epigenetic alterations, such as methylation of the promoter of cell cycle gene inhibitors with the resulting loss of its expression, have been frequently detected in liver cirrhosis with viral infection (4, 5). Continuous inflammation induces genetic or epigenetic alterations, or both, in hepatocytes, culminating in a preneoplastic condition. HCV itself is an oncogenic virus. HCV core protein or HCV NS5A protein has oncogenic potential function in animal models without inflammation (6, 7). *In vitro* studies have suggested that HCV protein modifies host immunity to sustain infection (8). The suppression of immunological response is attributed to the failure to eliminate neoplastic cells from the liver. These findings suggest that cooperation between virus-induced chronic inflammation and HCV coding proteins accelerates carcinogenesis in the liver.

Interferon (IFN) has potent antiviral activity against HCV. Antiviral therapy with pegylated IFN in combination with ribavirin produces a sustained virological response (SVR) in approximately 60% of patients with chronic hepatitis C (9, 10). Complete eradication of HCV by antiviral therapy is associated with a considerable reduction in the incidence of HCC (11, 12). Nevertheless, recent studies have shown that HCC develops in 2.5–4.2% of patients after eradication of HCV by IFN therapy (13–15). It is therefore important to delineate important features of HCC that develop after the elimination of HCV as compared with those established during sustained HCV infection. Makiyama *et al.* (15) speculated that cancer cells already exist in the liver before HCV eradication by IFN treatment. The integration of HBV DNA because of past HBV infections (16) or occult HCV infections (17) may be linked to SVR-HCC. However, the molecular mechanism leading to the development of SVR-HCC remains obscure.

In the present study, we compared genetic alterations in surgically resected specimens of HCCs between patients with SVR and those with continuous HCV infection. Our results might contribute to a better understanding of the molecular changes in

the liver of patients in whom HCC develops after the eradication of HCV.

Patients and methods

Patients

Thirteen consecutive patients who underwent surgical resection of HCC in Osaka City University Hospital after eradication of HCV by IFN monotherapy from 1998 June through 2007 July (SVR group) were studied (Table 1). One patient in the SVR group had two tumour nodules, both of which were examined. As a control, 44 HCV-RNA-positive patients with HCC were studied. Thus, 58 HCC samples and 57 noncancerous tissue samples were evaluated. One portion of each sample was frozen in liquid nitrogen immediately after resection and stored at − 80 °C until analysis. Total RNA and DNA were extracted from these portions by conventional methods as described previously (18). None of the patients had a history of exposure to aflatoxin B1, more than 30 g/day of alcohol intake, insulin administration, hereditary haemochromatosis or other liver diseases such as hepatitis B, autoimmune hepatitis and primary biliary cirrhosis. The activity of hepatitis and stage of fibrosis were determined according to a modified version of Desmet's classification in liver tissue specimens before IFN therapy and in noncancerous liver tissue obtained intra-operatively (19).

Table 1. Clinical characteristics of patients with sustained virological response-hepatocellular carcinoma and hepatitis C virus-hepatocellular carcinoma

	SVR-HCC	HCV-HCC	*P*-value
n	13	44	
Male/female	13/0	44/0	
Age	64.3 (55–73)	64.0 (34–79)	0.977
Anti-HCV(+)/ HCV-RNA(+)	13/0	44/44	
HBs antigen positivity	0	0	
IFN therapy	13	0	
ALT (IU/L)	35.0 (17–81)	73.2 (13–188)	0.0001
Diabetes mellitus With/without/ unknown	2/11/0	13/28/3	0.25
Alcohol habits Positive/negative/ unknown	5/8/0	23/17/4	0.23
Tumour differentiation Well/moderately/ poorly	0/4/10	5/20/19	0.066
Noncancerous liver Cirrhosis/noncirrhosis	4/9	20/24	0.34
Tumour diameter (mm) (average)	43.1 (12–125)	38.3 (10–180)	0.756
Extrahepatic metastasis	0	0	

ALT, alanine aminotransferase; HBs antigen, hepatitis B surface antigen; HCC, hepatocellular carcinoma; HCV, hepatitis C virus; IFN, interferon; SVR, sustained virological reaction.

Sequencing the displacement-loop region of mitochondrial DNA

Each DNA sample (50 ng) was subjected to amplification by polymerase chain reaction (PCR) with the use of overlapping sets of primers to screen the entire mitochondrial genome. To avoid coamplification of nuclear pseudogenes, the primers were selected with the use of mitochondrial DNA (mtDNA)-depleted cells established as described previously (2, 20). PCR (an initial incubation at 94 °C for 5 min, followed by 35 cycles of 94 °C for 30 s, 55 °C for 30 s and 72 °C for 1 min) was performed in a final volume of 50 µl with a GeneAmp PCR system 9600 (Perkin-Elmer Life Sciences Japan, Tokyo, Japan). Aberrant PCR products were purified with a QIAquick PCR purification kit (Qiagen, Tokyo, Japan) and sequenced with an Applied Biosystems DNA sequencer (Perkin-Elmer Life Sciences Japan) and a Dye Terminator Cycle Sequencing FS Ready Reaction kit (*Applied* Biosystems, Tokyo, Japan). The sequence of the displacement (D)-loop (nucleotides 100–600) was examined for all 57 patients with HCC. All mutations were confirmed by repeated DNA sequencing.

Direct sequencing for TP53

We directly sequenced exons 5 through 8 of TP53 genes, in which 98% of TP53 mutations are detected (21), in 58 tumours. One hundred nanograms of genomic DNA was subjected to 35 PCR cycles (94, 55 and 72 °C for 0.5, 0.5 and 1 min respectively) with rTaq DNA polymerase (TakaraBio Co. Ltd, Otsu, Japan). After the PCR products were purified with a QIAquick PCR purification kit, we sequenced the amplified products with a DNA sequencing system and a Dye Terminator Cycle Sequencing FS Ready Reaction kit.

Methylation-specific polymerase chain reaction

Bisulphite modification of genomic DNA was performed as described by Herman *et al.* (22). Briefly, 1 µg of DNA was denatured with NaOH, and 10 mM hydroquinone and 3 M sodium bisulphite were successively added to the mixture. The sample was incubated at 50 °C for 16 h. Modified DNA was purified with the use of Wizard DNA purification resin (Promega Corporation, Madison, WI, USA), followed by ethanol precipitation. DNA methylation patterns were determined by chemical modification of the unmethylated cytosines to uracil and subsequent PCR, using primers specific for either methylated or modified unmethylated DNA. The primers used in this study are shown in Table 2 (23, 24). The PCR amplification procedure has been described previously (5). Ten microlitres of each PCR product was loaded directly onto nondenaturing 2% agarose gels, stained with ethidium bromide and visualized under ultraviolet illumination.

Semiquantitative reverse-transcription polymerase chain reaction analysis

To investigate *p16* mRNA expression, we performed reverse-transcription PCR (RT-PCR) with total RNA from 35 tumours and 27 noncancerous lesions. Briefly, 1 µg of the RNA was used as a template to generate complementary DNA (cDNA) using random hexamers and reverse transcriptase. The cDNA was used for PCR amplification. Primer sequences were 5′-CCACCCCGC TTTCGTAGTTTT-3′ (upper primer) and 5′-TGCGAGGCTCG CAAGAAAT-3′ (lower primer) for *p16* and 5′-CCTCGCCTT TGCCGATCC-3′ (upper primer) and 5′-GGATCTTCATGAGG TAGTCAGTC-3′ (lower primer) for β-actin. The PCR procedure for *p16* consisted of one cycle at 95 °C for 12 min, 30 cycles at 95 °C for 30 s, 51 °C for 1 min and 72 °C for 30 s, and one cycle at

Table 2. Primers used for methylation-specific polymerase chain reaction

Gene		Sequence
p16	Unmethylated	5'-TTATTAGAGGGTGGGGTGGATTGT-3' (sense)
		5'-CAACCCCAAACCACAACCATAA-3' (antisense)
	Methylated	5'-TTATTAGAGGGTGGGGCGGATCGC-3' (sense)
		5'-GACCCCGAACCGCGACCGTAA-3' (antisense)
p15	Unmethylated	5'-TGTGATGTGTTTGTATTTTGTGGTT-3' (sense)
		5'-CCATACAATAACCAAACAACCAA-3' (antisense)
	Methylated	5'-GCGTTCGTATTTTGCGGTT-3' (sense)
		5'-CGTACAATAACCGAACGACCGA-3' (antisense)
p14	Unmethylated	5'-TTTTTGGTGTTAAAGGGTGGTGTAGT-3' (sense)
		5'-CACAAAAACCCTCACTCACAACAA-3' (antisense)
	Methylated	5'-GTGTTAAAGGGCGGCGTAGC-3' (sense)
		5'-AAAACCCTCACTCGCGACGA-3' (antisense)
RB		5'-CTTTGTATAGCCCCGTTAAGTG-3' (sense)
		5'-GTCATGAGGAATTAAACTGGGA-3' (antisense)
PTEN	Unmethylated	5'-GTGTTGGTGGAGGTAGTTGTTT-3' (sense)
		5'-ACCACTTAACTCTAAACCACAACCA-3' (antisense)
	Methylated	5'-TTCGTTCGTCGTCGTCGTATTT-3' (sense)
		5'-GCCGCTTAACTCTAAACCGCAACCG-3' (antisense)

72 °C for 3 min. That for β-actin consisted of one cycle at 94 °C for 3 min, 24 cycles at 95 °C for 30 s, 60 °C for 1 min and 72 °C for 30 s, and one cycle at 72 °C for 3 min. Ten microlitres of each PCR product was loaded directly onto nondenaturing 8% polyacrylamide gels, and the gels were stained with SYBR Greene (BioWhittaker Molecular Applications, Rockland, ME, USA) according to the manufacturer's protocol. The intensity of the bands was quantified by densitometry.

Statistical analysis

Age, tumour size, liver function and mtDNA mutations were compared between the two groups with the Mann–Whitney *U* test. Histological findings, diabetes mellitus, alcohol use, tumour differentiation, TP53 mutation and methylation status were compared between the two groups with the χ^2 test.

Ethical considerations

This study protocol complied with the ethical guidelines of the Declaration of Helsinki (1975) and was approved by the Ethics Committee of Osaka City University Graduate School of Medical.

Results

Histological findings in patients with sustained virological response

In patients with SVR, the period from the end of IFN treatment to hepatectomy for HCC ranged from 13 to 156 months. Histological examinations, performed in 11 of the 13 patients with SVR-HCCs, showed that the staging of hepatic fibrosis improved in five patients and the grade of hepatic activity improved in eight patients (Table 3).

Mitochondrial DNA mutations of hepatocellular carcinoma

Mutations of mtDNA were found in both HCC and noncancerous liver tissue. Previously, three mutation sites in mtDNA have been reported to be unique for the Japanese. Excluding these sites, we evaluated the average number of mtDNA mutations in D-loop lesions (Table 4). The average number of mtDNA mutations in D-loop lesions was 4.2 in 44 HCCs with HCV and 2.0 in 14 HCCs from SVR patients. The average number of mtDNA mutations in D-loop lesions was 2.8 in 44 noncancerous lesions with HCV and 1.3 in 13 noncancerous lesion from SVR patients. No specific mutation in mtDNA of SVR-HCC was found in the present study. The frequency of mtDNA mutations in HCC was significantly lower in SVR patients than in HCV patients ($P = 0.0021$). The frequency of mtDNA mutations was also lower in noncancerous livers of SVR patients ($P = 0.007$). In the present study, no regularity of mtDNA mutations was found in the D-loop region.

TP53 mutation analysis

TP53 mutations were detected in 12 (27.3%) of 44 HCCs with HCV (Table 4). In detail, TP53 was mutated in codon 123, TAT to TTC; codon 132, AAG to TTG; codon 133, ATG to TTG; codon 158, CGC to CTC; codon 189, GCC to GTC; codon 220, TAT to TGT; codon 246, ATG to GTG; codon 272, GAG to GTG; codon 275, TGT to TAT; and codon 271, CAT to CGT. Two cases were mutated by insertion in exons 5 and 8. The histological findings showed that HCCs with TP53 mutations consisted of seven moderately differentiated and five poorly differentiated HCCs. TP53 mutations were detected in two (14.3%) of 14 HCCs from the 13 patients in whom HCV was eradicated by IFN therapy. In detail, TP53 was mutated in codon 135, TGC to TGG and codon 242, TGC to TTC. The histological findings showed that HCCs with TP53 mutations in SVR patients consisted of two poorly differentiated HCCs.

Methylation pattern of hepatocellular carcinoma

In patients with HCV, hypermethylation of *p16*, *p15*, *p14*, *RB* and the *PTEN* promoter was, respectively, detected in 34 (77.3%), 13 (29.5%), 8 (18.2%), 12 (27.3%) and 11 (25.0%) of 44 HCCs and 13 (29.5%), 14 (31.8%), 4 (9.1%), 11 (25.0%) and 5 (11.4%) of 44 noncancerous liver samples (Fig. 1A). In patients with SVR, hypermethylation of *p16*, *p15*, *p14*, *RB* and the *PTEN* promoter was, respectively, detected in 14 (100%), 0 (0%), 0 (0%), 2 (14.3%) and 2 (14.3%) of 14 HCCs and 2 (15.4%), 0 (0%), 0 (0%), 2 (15.4%) and 0 (0%) of 13

Table 3. Clinical course of patients with sustained virological response-hepatocellular carcinoma

Case	Pre-IFN therapy				Span for carcinogenesis after IFN therapy (months)	At operation		
	Genotype	HCV-RNA	*F* factor	*A* factor		*F* factor	*A* factor	BMI
56	1b	1 MEq	2	2	45	2	1	23.7
101	2a	+	3	2	19	4	2	23.7
149	2a	1.1 MEq	4	3	20	4	2	23.6
196	2b	+	2	2	41	1	2	23.4
198	2a	0.4 MEq	2	2	103	1	1	21.5
200	2a	1.1 MEq	2	2	13	2	1	24.6
221	2a	0.9 MEq	2	3	80	2	2	18.1
268	Unknown	+	Unknown	Unknown	144	1	1	20.3
269	2a	0.4 MEq	2	3	156	0	0	23.6
271	1b	+	4	1	156	3	1	28.1
325	1b	300 KIU	3	2	15	2	1	25.2
327	2b	160 KIU	3	3	36	4	2	26.8
328	1b	+	Unknown	Unknown	14	4	2	27.6

BMI, body mass index; HCV, hepatitis C virus; HCC, hepatocellular carcinoma; IFN, interferon; SVR, sustained virological response.

Table 4. Comparison of mutation in the displacement-loop of mitochondrial DNA, mutation in TP53 and methylation between sustained virological response-hepatocellular carcinoma and hepatitis C virus-hepatocellular carcinoma

	SVR-HCC	HCV-HCC	*P*-value
Mean mutation number in D-loop of mtDNA	2.0	4.2	0.0021
TP53 mutation	14.3%	27.3%	0.322
Methylation			
p16	100.0%	77.3%	0.049
p15	0.0%	29.5%	0.021
p14	0.0%	18.2%	0.085
RB	14.3%	27.3%	0.322
PTEN	14.3%	25.0%	0.402

D-loop, displacement-loop; HCC, hepatocellular carcinoma; HCV, hepatitis C virus; mtDNA, mitochondrial DNA; SVR, sustained virological response.

noncancerous liver samples (Fig. 1B). Methylation of *p14*, *p15*, *RB* and *PTEN* was thus slightly but not significantly more frequent in HCV-HCC than in SVR-HCC.

Expression of *p16* mRNA in hepatocellular carcinoma

Expression of *p16* mRNA was examined in 29 patients with HCV-HCC and six with SVR-HCC. In six SVR-HCCs with *p16* promoter methylation, *p16* mRNA expression was lower than that in the noncancerous liver (Fig. 2). In 29 HCV-HCCs with *p16* methylation, *p16* mRNA expression was lower than that in HCC without *p16* methylation.

Discussion

In agreement with previous studies, all patients with SVR-HCC were males in the present study (15), suggesting that sex-related factors have a role in SVR-HCC. We, therefore, studied male patients with HCV-HCC and matched subjects with SVR-HCC. First of all, mtDNA mutations were frequent in HCC as well as in noncancerous liver tissues from patients with HCV (2, 25). Chronic viral inflammation induces ROS production, followed by mtDNA damage in the liver, which is speculated to contribute to hepatocarcinogenesis (25). In contrast to mtDNA mutations, the frequency of mtDNA mutations was low in SVR liver. Histological examination of noncancerous liver tissue showed that persistent inflammation was minimal or absent in SVR patients. Nishikawa *et al.* reported that IFN therapy reduces the frequency of mtDNA mutations in the liver of patients with chronic hepatitis C. In their study, a reduced frequency of mtDNA mutations was detected only in patients whose transaminases were normalized by IFN therapy in association with HCV elimination (26). Our study also showed that the frequency of mtDNA mutations was reduced in the liver of SVR patients. In the present study, no patient with HCV-HCC received IFN. Therefore, we could not exactly clarify which factor was more closely related to fewer mtDNA mutations in SVR-HCC, IFN or HCV eradication. However, we speculate that chronic inflammation was not related to the development of HCC in SVR patients.

Destruction of tumour suppressor gene function is thought to be a critical step in carcinogenesis. Previous studies showed that TP53 mutations were detected in 27% (21) and 38.3% (27) of HCCs with viral infection. These high rates were apparently related to the late stage of hepatocarcinogenesis. In agreement with these previous reports, TP53 was mutated in seven moderately differentiated HCC and five poorly differentiated HCC (27.7%) in the 44 patients with HCV in our study. To our knowledge, no previous study has reported TP53 mutations in SVR-HCC. We found two TP53 mutations in 14 SVR-HCC, including dedifferentiated lesions. mtDNA damage induced by chronic viral hepatitis correlates with genomic injury. It was speculated that a decrease in mtDNA mutations followed loss of TP53 mutations. Although the small number of the SVR-HCCs examined in our study precludes firm conclusions, TP53 alterations might differ between SVR-HCC and HCV-HCC.

Next, we showed epigenetic alterations in both HCV-HCC and SVR-HCC. Previous studies have reported that *p16*, *p15*,